STATISTICS, OPTIMIZATION AND INFORMATION COMPUTING
Stat., Optim. Inf. Comput., Vol. **16**, July 2026, pp 219–246.
Published online in International Academic Press (www.IAPress.org)

The New Heavy-tailed Weibull Exponentiated Half Logistic-G Family of Distributions: Properties, Actuarial Measures and Inference

Wilbert Nkomo[1,2*], Broderick Oluyede[1], Thatayaone Moakofi[3], Fastel Chipepa[1], Wellington Charumbira[1,4]

[1]*Department of Mathematics and Statistical Sciences, Botswana International University of Science and Technology, Botswana*
[2]*Department of Applied Statistics, Manicaland State University of Applied Sciences, Mutare, Zimbabwe*
[3]*Department of Statistics, University of Botswana, Gaborone, Botswana*
[4]*Department of Applied Mathematics and Statistics, Midlands State University, Gweru, Zimbabwe*

Abstract Accurate statistical modeling of complex real-world data, characterized by heavy tails, skewness, and non-monotonic hazard rates, presents a significant challenge that often exceeds the capabilities of traditional distributions. To address this, we introduce the Heavy-Tailed Weibull Exponentiated Half Logistic-G (HT-W-EHL-G) family of distributions, a novel flexible framework that synthesizes extreme-value robustness with versatile hazard rate shapes. This paper derives the fundamental statistical properties of the proposed family and establishes six estimation methods, whose efficiency is verified via Monte Carlo simulation. The model's practical utility is demonstrated by its robustness to censored data, a critical requirement in survival and reliability analysis, and its direct applicability for computing key actuarial risk measures, including Value at Risk (VaR) and Tail Value at Risk (TVaR). Extensive empirical analyses across diverse domains confirm the model's efficacy and statistically significant superiority in goodness-of-fit over established benchmarks.

Keywords Heavy-tailed distributions, Hazard rate function, Risk measures, Maximum likelihood estimation, Simulations.

AMS 2010 subject classifications 62E30; 60E05; 62E15

DOI: 10.19139/soic-2310-5070-3125

1. Introduction

Probability distributions are fundamental for modeling real-world phenomena across diverse fields including finance, engineering, and medical sciences. Recent advancements in distribution theory have focused on developing increasingly flexible models to capture complex data behaviors such as skewness, heavy tails, and multimodal patterns. The accurate assessment of tail risk in modern datasets, which often contain extreme outliers, necessitates robust modeling frameworks that surpass traditional distributions including the Pareto, normal, exponential, and Weibull distributions. This need has driven the adoption of advanced generalized and composite models.

A major advancement has been the development of generator techniques to extend existing distributions. Notable frameworks include: (1) the new Weibull-G generator by Tahir et al. [22], which introduces enhanced flexibility for lifetime data modeling; (2) the T-X family by Alzaatreh et al. [3], providing a generalized approach for distribution generation; and (3) the exponentiated half logistic-G (EHL-G) distribution by Cordeiro et al. [8], offering improved capability for skewed data analysis. These generators significantly expand statistical modeling capabilities through additional shape and scale parameters that enhance adaptability to diverse real-world scenarios.

*Correspondence to: Wilbert Nkomo (Email: wilbert.nkomo@staff.msuas.ac.zw). Department of Applied Statistics, Manicaland State University of Applied Sciences, Stair Guthrie Road, P. Bag 7001, Fernhill, Mutare, Zimbabwe.

ISSN 2310-5070 (online) ISSN 2311-004X (print)

Particularly relevant to this study is the type I heavy-tailed-G distribution pioneered by Zhao et al. [26], which has demonstrated superior performance in modeling heavy-tailed phenomena. Heavy-tailed distributions have gained prominence due to their ability to model extreme events, especially crucial in risk assessment, reliability engineering, and actuarial science. Recent works highlighting the growing interest in this area include: the heavy-tailed beta-power transformed Weibull distribution by Zhao et al. [25], the Topp-Leone type I heavy-tailed-G power series class by Nkomo et al. [16], the heavy-tailed exponential distribution by Afify et al. [1], the heavy-tailed log-logistic distribution by Teamah et al. [23], the type I heavy-tailed odd power generalized Weibull-G family by Moakofi et al. [14], the exponentiated half logistic-type I heavy-tailed-G family by Gwazane et al. [11], the Ristić -Balakrishnan-heavy-tailed-type II Topp-Leone-G family by Warahena-Liyanage et al. [24], and the type I heavy-tailed-odd Burr III-G family by Nkomo et al. [17]. These distributions provide robust frameworks for analyzing datasets with rare but high-impact events such as financial crashes, catastrophic failures, or extreme survival times.

Building on these advancements, we propose the heavy-tailed Weibull-exponentiated half logistic-G (HT-W-EHL-G) family of distributions (FoD), which combines the flexibility of the Weibull exponentiated half logistic-G (W-EHL-G) framework by Peter et al. [19] with the heavy-tailed properties introduced by Zhao et al. [26]. This new FoD not only generalizes several existing models but also offers enhanced capability to represent diverse hazard rate shapes including increasing, decreasing, bathtub, and inverted bathtub patterns, making it suitable for a wide range of applications.

The heavy-tailed-G (HT-G) FoD proposed by Zhao et al. [26] has the cumulative distribution function (cdf)

$$F(z;\theta,\Upsilon) = 1 - \left(\frac{\bar{G}(z;\Upsilon)}{1-(1-\theta)G(z;\Upsilon)}\right)^{\theta} \tag{1}$$

and probability density function (pdf)

$$f(z;\theta,\Upsilon) = \frac{\theta^2 g(z;\Upsilon)\left[\bar{G}(z;\Upsilon)\right]^{\theta-1}}{\left[1-(1-\theta)G(z;\Upsilon)\right]^{\theta+1}}, \tag{2}$$

where $\theta > 0$ is a tilt parameter, $z > 0$, $\bar{G}(z;\Upsilon) = 1 - G(z;\Upsilon)$ and Υ is the parameter vector from the parent distribution $G(\cdot)$.

The Weibull exponentiated half logistic-G (W-EHL-G) FoD pioneered by Peter et al. [19] (see also Moakofi et al. [15]) has the cdf

$$F(z;\alpha,\beta,\Upsilon) = 1 - \exp\left(-\left[-\log\left(1-\left(\frac{G(z;\Upsilon)}{1+\bar{G}(z;\Upsilon)}\right)^{\alpha}\right)\right]^{\beta}\right) \tag{3}$$

and pdf

$$\begin{aligned} f(z;\alpha,\beta,\Upsilon) &= \frac{2\alpha\beta g(z;\Upsilon)}{\left(1+\bar{G}(z;\Upsilon)\right)^2}\exp\left(-\left[-\log\left(1-\left(\frac{G(z;\Upsilon)}{1+\bar{G}(z;\Upsilon)}\right)^{\alpha}\right)\right]^{\beta}\right) \\ &\times \left[-\log\left(1-\left(\frac{G(z;\Upsilon)}{1+\bar{G}(z;\Upsilon)}\right)^{\alpha}\right)\right]^{\beta-1}\left(1-\left(\frac{G(z;\Upsilon)}{1+\bar{G}(z;\Upsilon)}\right)^{\alpha}\right)^{-1}\left(\frac{G(z;\Upsilon)}{1+\bar{G}(z;\Upsilon)}\right)^{\alpha-1}, \end{aligned}$$

where $\alpha, \beta > 0$ are shape parameters, $\bar{G}(z;\Upsilon) = 1 - G(z;\Upsilon)$, and Υ is a parameter vector from the parent distribution $G(\cdot)$.

Extending from the established but distinct strengths of the W-EHL-G and HT-G families, this study addresses a critical gap in distribution theory by developing a unified generative framework. The proposed HT-W-EHL-G family directly synthesizes the broad hazard rate versatility of the former with the robust tail-domain control of the latter, providing a mathematically integrated model designed for the rigorous characterization of modern, complex datasets exhibiting both multimodal hazard profiles and significant extreme-value behavior.

The paper proceeds as follows: Section 2 introduces the generalized family, detailing its sub-families and special cases. Section 3 derives key statistical properties including density expansion, moments, probability weighted

moments and entropy. Section 4 discusses various parameter estimation methods for both uncensored and censored datasets. Section 5 validates the framework's reliability through Monte Carlo simulations across varying sample sizes. Section 6 integrates various risk measures with numerical simulations to quantify extreme-event behavior. Section 7 demonstrates the model's superiority through empirical case studies including stress-rupture lifetimes, material fracture toughness, and cancer remission data. Finally, Section 8 synthesizes the study's contributions and suggests directions for future research.

2. The new family and its properties

Substituting the parent cdf in Equation (1) with the WEHL-G cdf yields the HT-WEHL-G FoD with cdf, survival function, pdf and hazard rate function (hrf) given by

$$F(z;\alpha,\beta,\theta,\Upsilon) = 1-\left(\frac{\exp\left(-\left[-\log\left(1-\left(\frac{G(z;\Upsilon)}{1+\bar{G}(z;\Upsilon)}\right)^{\alpha}\right)\right]^{\beta}\right)}{1-(1-\theta)\left[1-\exp\left(-\left[-\log\left(1-\left(\frac{G(z;\Upsilon)}{1+\bar{G}(z;\Upsilon)}\right)^{\alpha}\right)\right]^{\beta}\right)\right]}\right)^{\theta}, \tag{4}$$

$$S(z;\alpha,\beta,\theta,\Upsilon) = \left(\frac{\exp\left(-\left[-\log\left(1-\left(\frac{G(z;\Upsilon)}{1+\bar{G}(z;\Upsilon)}\right)^{\alpha}\right)\right]^{\beta}\right)}{1-(1-\theta)\left[1-\exp\left(-\left[-\log\left(1-\left(\frac{G(z;\Upsilon)}{1+\bar{G}(z;\Upsilon)}\right)^{\alpha}\right)\right]^{\beta}\right)\right]}\right)^{\theta}, \tag{5}$$

$$\begin{aligned} f(z;\alpha,\beta,\theta,\Upsilon) &= \frac{2\alpha\beta\theta^2 g(z;\Upsilon)}{\left(1+\bar{G}(z;\Upsilon)\right)^2}\left[-\log\left(1-\left(\frac{G(z;\Upsilon)}{1+\bar{G}(z;\Upsilon)}\right)^{\alpha}\right)\right]^{\beta-1}\left(1-\left(\frac{G(z;\Upsilon)}{1+\bar{G}(z;\Upsilon)}\right)^{\alpha}\right)^{-1} \\ &\times \left[\exp\left(-\left[-\log\left(1-\left(\frac{G(z;\Upsilon)}{1+\bar{G}(z;\Upsilon)}\right)^{\alpha}\right)\right]^{\beta}\right)\right]^{\theta}\left(\frac{G(z;\Upsilon)}{1+\bar{G}(z;\Upsilon)}\right)^{\alpha-1} \\ &\times \left(1-(1-\theta)\left[1-\exp\left(-\left[-\log\left(1-\left(\frac{G(z;\Upsilon)}{1+\bar{G}(z;\Upsilon)}\right)^{\alpha}\right)\right]^{\beta}\right)\right]\right)^{-(\theta+1)} \end{aligned} \tag{6}$$

and

$$\begin{aligned} h(z;\alpha,\beta,\theta,\Upsilon) &= \frac{2\alpha\beta\theta^2 g(z;\Upsilon)}{\left(1+\bar{G}(z;\Upsilon)\right)^2}\left[-\log\left(1-\left(\frac{G(z;\Upsilon)}{1+\bar{G}(z;\Upsilon)}\right)^{\alpha}\right)\right]^{\beta-1}\left(1-\left(\frac{G(z;\Upsilon)}{1+\bar{G}(z;\Upsilon)}\right)^{\alpha}\right)^{-1} \\ &\times \left[\exp\left(-\left[-\log\left(1-\left(\frac{G(z;\Upsilon)}{1+\bar{G}(z;\Upsilon)}\right)^{\alpha}\right)\right]^{\beta}\right)\right]^{\theta}\left(\frac{G(z;\Upsilon)}{1+\bar{G}(z;\Upsilon)}\right)^{\alpha-1} \\ &\times \left(1-(1-\theta)\left[1-\exp\left(-\left[-\log\left(1-\left(\frac{G(z;\Upsilon)}{1+\bar{G}(z;\Upsilon)}\right)^{\alpha}\right)\right]^{\beta}\right)\right]\right)^{-(\theta+1)} \\ &\times \left(\frac{\exp\left(-\left[-\log\left(1-\left(\frac{G(z;\Upsilon)}{1+\bar{G}(z;\Upsilon)}\right)^{\alpha}\right)\right]^{\beta}\right)}{1-(1-\theta)\left[1-\exp\left(-\left[-\log\left(1-\left(\frac{G(z;\Upsilon)}{1+\bar{G}(z;\Upsilon)}\right)^{\alpha}\right)\right]^{\beta}\right)\right]}\right)^{-\theta}, \end{aligned} \tag{7}$$

respectively for $\alpha,\beta,\theta,z>0$ and parameter vector Υ.

2.1. HT-W-EHL-G sub-families

Table 1 presents various sub-families associated with the HT-W-EHL-G FoD, accompanied by their corresponding nomenclature.

Table 1. Sub-families of HT-W-EHL-G FoD and their nomenclature

α	β	θ	Resultant Distribution	Distribution Nomenclature
1	-	-	$F(z;\beta,\theta,\Upsilon)=1-\left(\frac{\exp\left(-\left[-\log\left(1-\left(\frac{G(z;\Upsilon)}{1+G(z;\Upsilon)}\right)\right)\right]^{\beta}\right)}{1-(1-\theta)\left[1-\exp\left(-\left[-\log\left(1-\left(\frac{G(z;\Upsilon)}{1+G(z;\Upsilon)}\right)\right)\right]^{\beta}\right)\right]}\right)^{\theta}$	Heavy-tailed Weibull half logistic-G FoD
-	1	-	$F(z;\alpha,\theta,\Upsilon)=1-\left(\frac{1-\left(\frac{G(z;\Upsilon)}{1+G(z;\Upsilon)}\right)^{\alpha}}{1-(1-\theta)\left[\left(\frac{G(z;\Upsilon)}{1+G(z;\Upsilon)}\right)^{\alpha}\right]}\right)^{\theta}$	A new heavy-tailed exponentiated half logistic FoD
-	-	1	$F(z;\alpha,\beta,\Upsilon)=1-\left(\exp\left(-\left[-\log\left(1-\left(\frac{G(z;\Upsilon)}{1+G(z;\Upsilon)}\right)^{\alpha}\right)\right]^{\beta}\right)\right)$	Weibull exponentiated half logistic-G FoD (Peter et al. [19]
1	1	-	$F(z;\alpha,\theta,\Upsilon)=1-\left(\frac{1-\left(\frac{G(z;\Upsilon)}{1+G(z;\Upsilon)}\right)}{1-(1-\theta)\left(\frac{G(z;\Upsilon)}{1+G(z;\Upsilon)}\right)}\right)^{\theta}$	A new heavy-tailed half logistic-G FoD
-	1	1	$F(z;\alpha,\Upsilon)=\left(\frac{G(z;\Upsilon)}{1+G(z;\Upsilon)}\right)^{\alpha}$	Exponentiated half logistic-G FoD (Cordeiro et al. [8])
1	-	1	$F(z;\beta,\Upsilon)=1-\exp\left(-\left[-\log\left(1-\left(\frac{G(z;\Upsilon)}{1+G(z;\Upsilon)}\right)\right)\right]^{\beta}\right)$	Weibull half logistic-G FoD (Peter et al. [19])
1	1	1	$F(z;\Upsilon)=\frac{G(z;\Upsilon)}{1+G(z;\Upsilon)}$	half logistic-G FoD (Cordeiro et al. [8])

2.2. Particular cases

This subsection presents some particular cases of HT-W-EHL-G FoD by specifying $G(z;\Upsilon)$ and $g(z;\Upsilon)$ in Equations (4) and (6). The Lindley, Weibull and Burr XII distributions serve as baseline distributions.

2.2.1. Heavy-tailed Weibull exponentiated half logistic-Lindley (HT-W-EHL-LIN) distribution: Considering the Lindley distribution with the cdf and pdf given by $G(z;c)=1-\left(1+\frac{cz}{1+c}\right)\exp(-cz)$ and $g(z;c)=\frac{c^2}{1+c}(1+z)\exp(-cz)$ as baseline distribution, for $z,c>0$, we have the HT-W-EHL-LIN distribution with cdf

$$F(z;\alpha,\beta,\theta,c) = 1-\left(\frac{\exp\left(-\left[-\log\left(1-(L_G(z;c))^{\alpha}\right)\right]^{\beta}\right)}{1-(1-\theta)\left[1-\exp\left(-\left[-\log\left(1-(L_G(z;c))^{\alpha}\right)\right]^{\beta}\right)\right]}\right)^{\theta}$$

and pdf

$$\begin{aligned} f(z;\alpha,\beta,\theta,c) &= \frac{2\alpha\beta\theta^2\frac{c^2}{1+c}(1+z)\exp(-cz)}{\left(1+\left(1+\frac{cz}{1+c}\right)\exp(-cz)\right)^2}\left[-\log\left(1-(L_G(z;c))^{\alpha}\right)\right]^{\beta-1}\left(1-(L_G(z;c))^{\alpha}\right)^{-1} \\ &\times \left[\exp\left(-\left[-\log\left(1-(L_G(z;c))^{\alpha}\right)\right]^{\beta}\right)\right]^{\theta}(L_G(z;c))^{\alpha-1} \\ &\times \left(1-(1-\theta)\left[1-\exp\left(-\left[-\log\left(1-(L_G(z;c))^{\alpha}\right)\right]^{\beta}\right)\right]\right)^{-(\theta+1)}, \end{aligned}$$

for $\alpha,b,\beta,c,z>0$, where $L_G(z;c)=\frac{1-\left(1+\frac{cz}{1+c}\right)\exp(-cz)}{1+\left(1+\frac{cz}{1+c}\right)\exp(-cz)}$. The hrf is

$$\begin{aligned} h(z;\alpha,\beta,\theta,c) &= \frac{2\alpha\beta\theta^2\frac{c^2}{1+c}(1+z)\exp(-cz)}{\left(1+\left(1+\frac{cz}{1+c}\right)\exp(-cz)\right)^2}\left[-\log\left(1-(L_G(z;c))^{\alpha}\right)\right]^{\beta-1}\left(1-(L_G(z;c))^{\alpha}\right)^{-1} \\ &\times (L_G(z;c))^{\alpha-1}\left(1-(1-\theta)\left[1-\exp\left(-\left[-\log\left(1-(L_G(z;c))^{\alpha}\right)\right]^{\beta}\right)\right]\right)^{-1}. \end{aligned}$$

In Figure 1, the HT-W-EHL-LIN distribution can exhibit unimodal, reversed-J, and positively skewed densities with bathtub, inverted bathtub, increasing, and decreasing hazard rates.

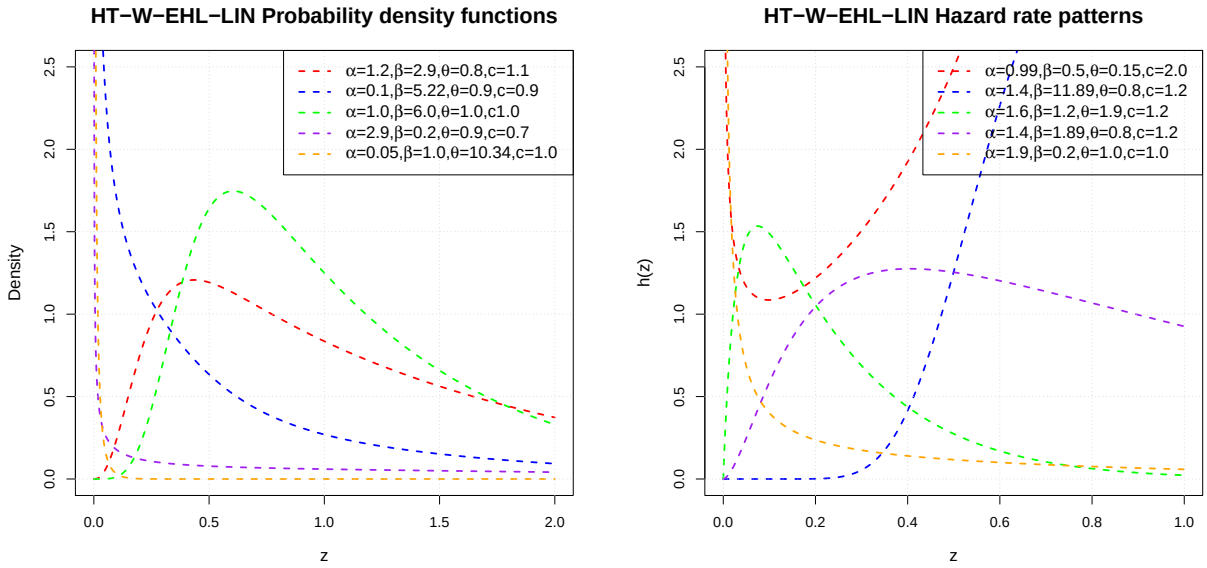

Figure 1. Plots of pdf and hrf for HT-W-EHL-LIN distribution

In Figure 2, a set of 3D plots illustrates the variability in skewness and kurtosis characteristics of the HT-W-EHL-LIN distribution. The plots demonstrate that fixing different parameter combinations produces varying degrees of skewness and peakedness. Key observations from the plots include:

- When θ and c are fixed, Figure 2 shows that kurtosis and skewness decrease as α and β increase in the HT-W-EHL-LIN distribution.
- Keeping α and β fixed, Figure 2 demonstrates that higher values of θ and c lead to an increase in both kurtosis and skewness for HT-W-EHL-LIN distribution.

2.2.2. Heavy-tailed Weibull exponentiated half logistic-Weibull (HT-W-EHL-W) distribution: The Weibull distribution has cdf $G(z;d) = 1 - \exp(-z^d)$, and pdf $g(z;d) = dz^{d-1}\exp(-z^d)$, for $z, d > 0$. If the Weibull distribution is applied to the HT-W-EHL-G distribution as baseline, we have the HT-W-EHL-W distribution with cdf

$$F(z;\alpha,\beta,\theta,d) = 1 - \left(\frac{\exp\left(-\left[-\log\left(1-(W_B(z;d))^{\alpha}\right)\right]^{\beta}\right)}{1-(1-\theta)\left[1-\exp\left(-\left[-\log\left(1-(W_B(z;d))^{\alpha}\right)\right]^{\beta}\right)\right]}\right)^{\theta}$$

and pdf

$$\begin{aligned} f(z;\alpha,\beta,\theta,d) &= \frac{2\alpha\beta\theta^2 dz^{d-1}\exp(-z^d)}{\left(1+\exp(-z^d)\right)^2}\left[-\log\left(1-(W_B(z;d))^{\alpha}\right)\right]^{\beta-1}\left(1-(W_B(z;d))^{\alpha}\right)^{-1} \\ &\times \left[\exp\left(-\left[-\log\left(1-(W_B(z;d))^{\alpha}\right)\right]^{\beta}\right)\right]^{\theta}(W_B(z;d))^{\alpha-1} \\ &\times \left(1-(1-\theta)\left[1-\exp\left(-\left[-\log\left(1-(W_B(z;d))^{\alpha}\right)\right]^{\beta}\right)\right]\right)^{-(\theta+1)}, \end{aligned}$$

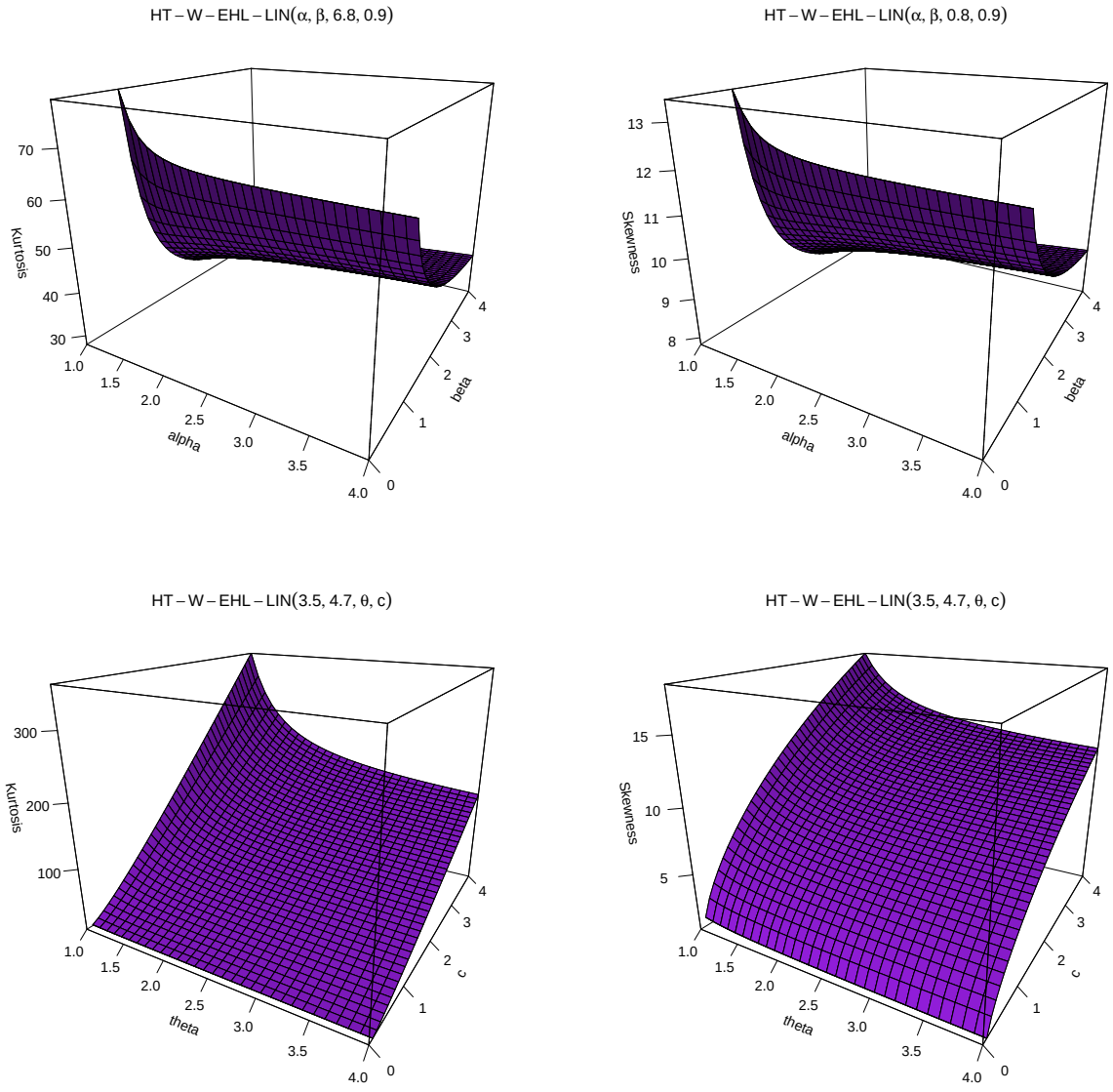

Figure 2. HT-W-EHL-LIN kurtosis and skewness plots for selected parameter values

for $\alpha, \beta, \theta, d, z > 0$, where $W_B(z;d) = \frac{1-\exp(-z^d)}{1+\exp(-z^d)}$. The hrf is

$$\begin{aligned} h(z;\alpha,\beta,\theta,d) &= \frac{2\alpha\beta\theta^2 dz^{d-1}\exp(-z^d)}{\left(1+\exp(-z^d)\right)^2}\left[-\log\left(1-(W_B(z;d))^\alpha\right)\right]^{\beta-1}\left(1-(W_B(z;d))^\alpha\right)^{-1} \\ &\times (W_B(z;d))^{\alpha-1}\left(1-(1-\theta)\left[1-\exp\left(-\left[-\log\left(1-(W_B(z;d))^\alpha\right)\right]^\beta\right)\right]\right)^{-1}. \end{aligned}$$

The density plots in Figure 3 demonstrate the adaptability of the HT-WEHL-W distribution in accommodating diverse datasets, including those that are positively skewed, negatively skewed, nearly symmetric, J and reversed-J shaped. Similarly, the hrf plot demonstrates its effectiveness in capturing patterns such as decreasing, increasing, and inverted bathtub-shaped shapes.

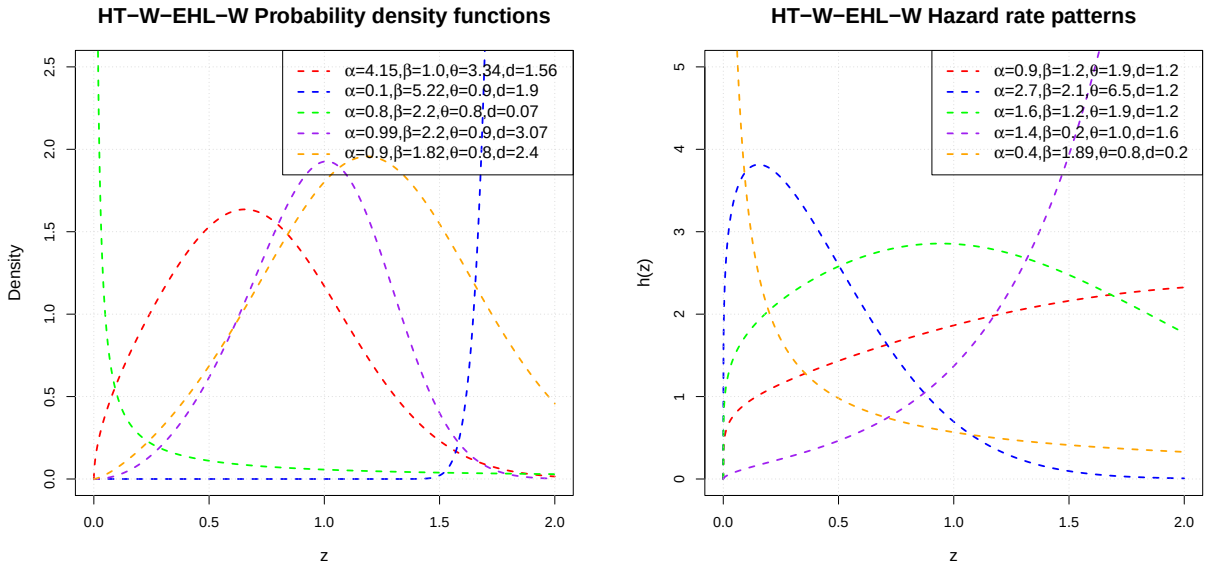

Figure 3. Plots showing the pdf and hrf for the HT-W-EHL-W distribution

In Figure 4, a set of 3D plots illustrates the variability in skewness and kurtosis characteristics of the HT-W-EHL-W distribution. The plots reveal that fixing varying combinations of parameters yield distinct levels of skewness and peakedness. The following observations can be drawn from the plots:

- Under fixed values of θ and d, the shape parameters α and β act as primary determinants of the distribution's asymmetry and tail behavior, as quantified by its kurtosis and skewness.
- If α and θ are held constant, a leptokurtic behaviour and positive skewness with increasing β and d for the HT-W-EHL-W distribution is exhibited.

2.2.3. Heavy-tailed Weibull exponentiated half logistic-Burr XII (HT-W-EHL-BXII) distribution: The Burr XII distribution is defined by the cdf $G(z;c,k) = 1-(1+z^c)^{-k}$ and pdf $g(z;c,k) = \frac{ckz^{c-1}}{(1+z^c)^{k+1}}$, where $z,c,k>0$. Employing the Burr XII as the baseline distribution to the HT-W-EHL-G FoD, we have the HT-W-EHL-BXII. The HT-W-EHL-BXII distribution has cdf

$$F(z;\alpha,\beta,\theta,c,k) = 1-\left(\frac{\exp\left(-\left[-\log\left(1-B_B(z;c,k)\right)\right]^{\beta}\right)}{1-(1-\theta)\left[1-\exp\left(-\left[-\log\left(1-B_B(z;c,k)\right)\right]^{\beta}\right)\right]}\right)^{\theta},$$

and pdf

$$\begin{aligned} f(z;\alpha,\beta,\theta,c,k) &= \frac{2\alpha\beta\theta^2 ckz^{c-1}}{(1+z^c)^{k+1}\left(1+(1+z^c)^{-k}\right)^2}\left[-\log\left(1-B_B(z;c,k)\right)\right]^{\beta-1} \\ &\times \left(1-B_B(z;c,k)\right)^{-1}\left(\frac{1-(1+z^c)^{-k}}{1+(1+z^c)^{-k}}\right)^{\alpha-1}\left[\exp\left(-\left[-\log\left(1-B_B(z;c,k)\right)\right]^{\beta}\right)\right]^{\theta} \\ &\times \left(1-(1-\theta)\left[1-\exp\left(-\left[-\log\left(1-B_B(z;c,k)\right)\right]^{\beta}\right)\right]\right)^{-(\theta+1)}, \end{aligned}$$

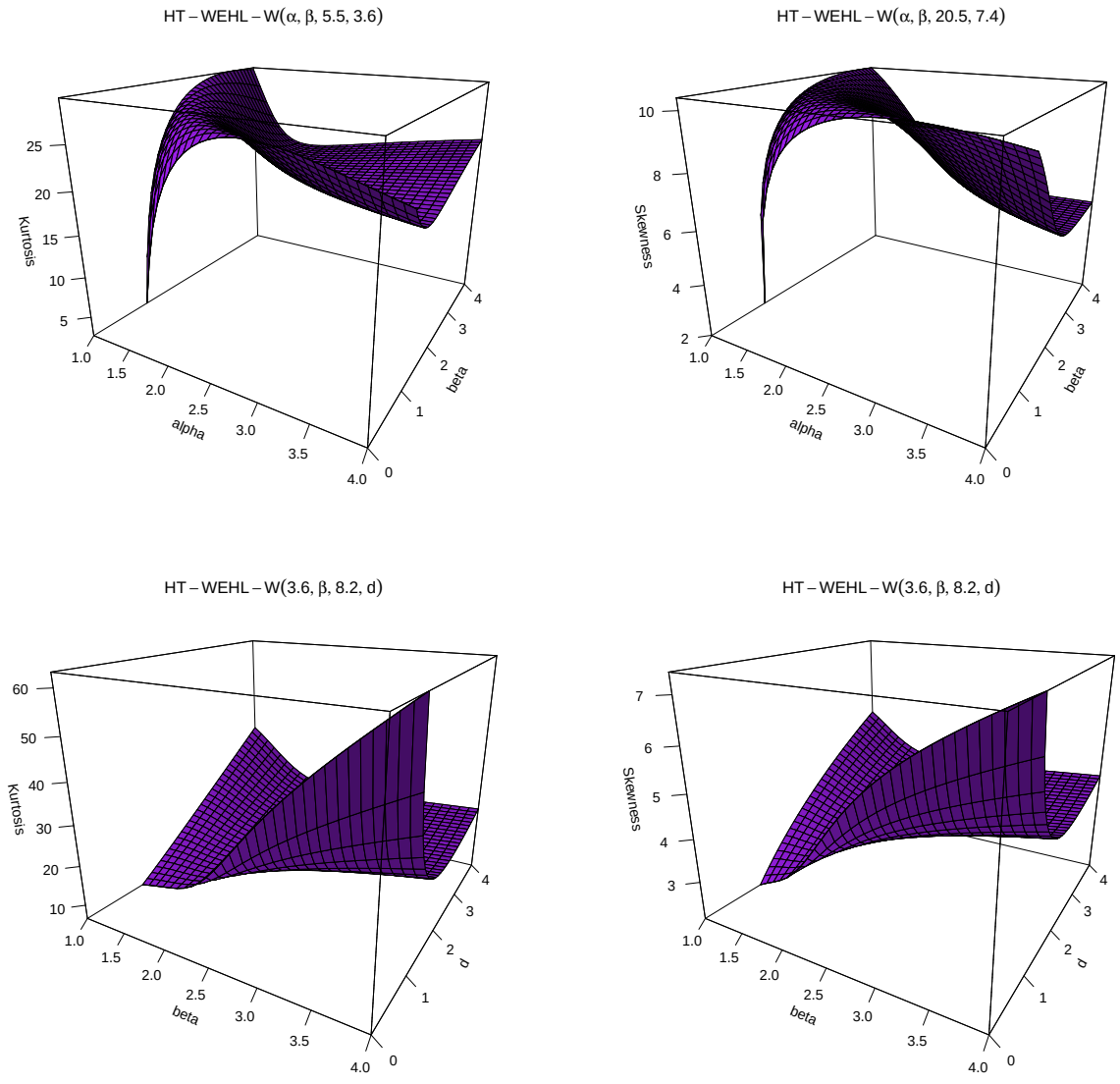

Figure 4. Kurtosis and skewness plots for the HT-W-EHL-W distribution

for $\alpha, \beta, \theta, c, k, z > 0$, where $B_B(z; c, k) = \left(\frac{1-(1+z^c)^{-k}}{1+(1+z^c)^{-k}}\right)^{\alpha}$. The hrf is

$$\begin{aligned} h(z;\alpha,\beta,\theta,c,k) &= \frac{2\alpha\beta\theta^2 ckz^{c-1}}{(1+z^c)^{k+1}\left(1+(1+z^c)^{-k}\right)^2}\left[-\log\left(1-B_B(z;c,k)\right)\right]^{\beta-1} \\ &\times \left(1-B_B(z;c,k)\right)^{-1}\left(\frac{1-(1+z^c)^{-k}}{1+(1+z^c)^{-k}}\right)^{\alpha-1} \\ &\times \left(1-(1-\theta)\left[1-\exp\left(-\left[-\log\left(1-B_B(z;c,k)\right)\right]^{\beta}\right)\right]\right)^{-1}. \end{aligned}$$

A particularly compelling feature of the HT-W-EHL-BXII distribution is its ability to generate special distributions through parameter simplification. Specifically, when $k = 1$, the heavy-tailed Weibull exponentiated half logistic-log-logistic (HT-W-EHL-LLoG) distribution emerges as a special case, while setting $c = 1$ yields the heavy-tailed Weibull exponentiated half logistic-Lomax (HT-W-EHL-Lom) distribution. These derivations elegantly demonstrate the flexibility of the HT-W-EHL-G framework, enabling tailored modeling for distinct data behaviors and expanding its applicability to diverse statistical scenarios.

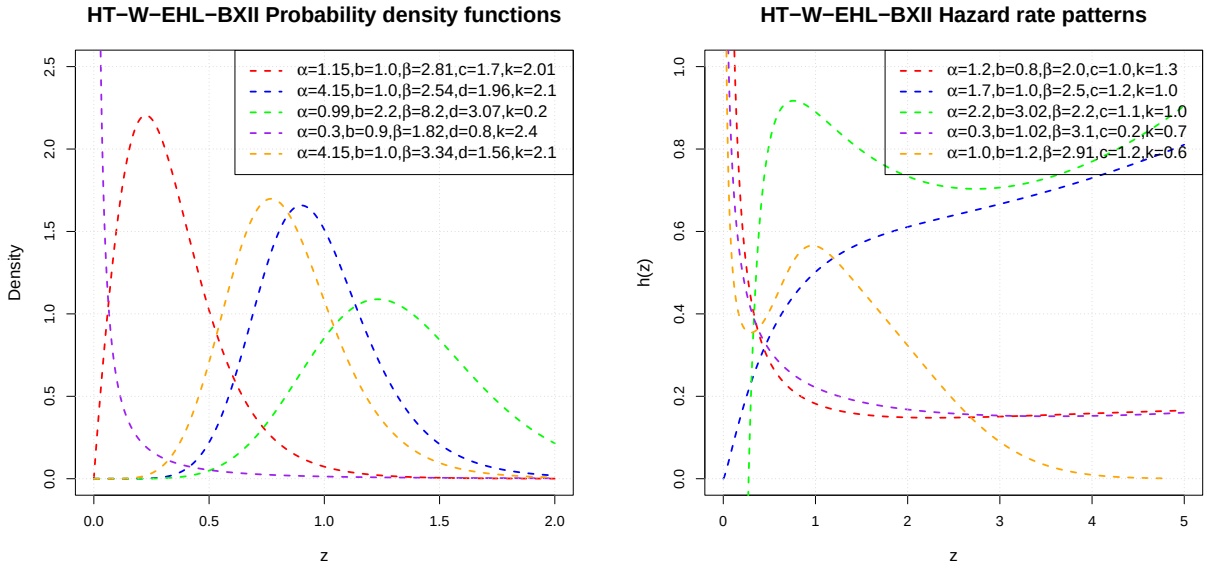

Figure 5. Density and hrf plots for the HT-W-EHL-BXII distribution

The density plots in Figure 5 illustrate the HT-WEHL-BXII distribution's capacity to model a broad spectrum of data configurations, including positively skewed, negatively skewed, approximately symmetric, and reversed-J-shaped probability structures. This highlights its robust flexibility for empirical applications. The hrf plots exhibit its dynamic adaptability in characterizing complex failure rate behaviors, such as monotonically decreasing, monotonically increasing, bathtub-to-inverted bathtub transitions, and inverted bathtub-to-bathtub transitions.
Figure 6 presents 3D plots characterizing the joint variability of skewness and kurtosis for the HT-W-EHL-BXII distribution. The findings emerging from the analysis are summarized as follows:

- After controlling for α, β and k, varying levels of kurtosis and skewness are observed with increasing b and c for the HT-W-EHL-BXII distribution.
- If b, c and k are held constant, kurtosis and skewness increase with increasing α and β for the HT-W-EHL-BXII distribution.

3. Statistical properties

Series expansions of density functions provide powerful techniques for approximating, estimating, and computing complex distributions. Additionally, statistical properties such as the quantile function (QF), entropy, moments, moment generating functions (mgfs), and incomplete moments are fundamental tools for characterizing, analyzing and comparing probability distributions.

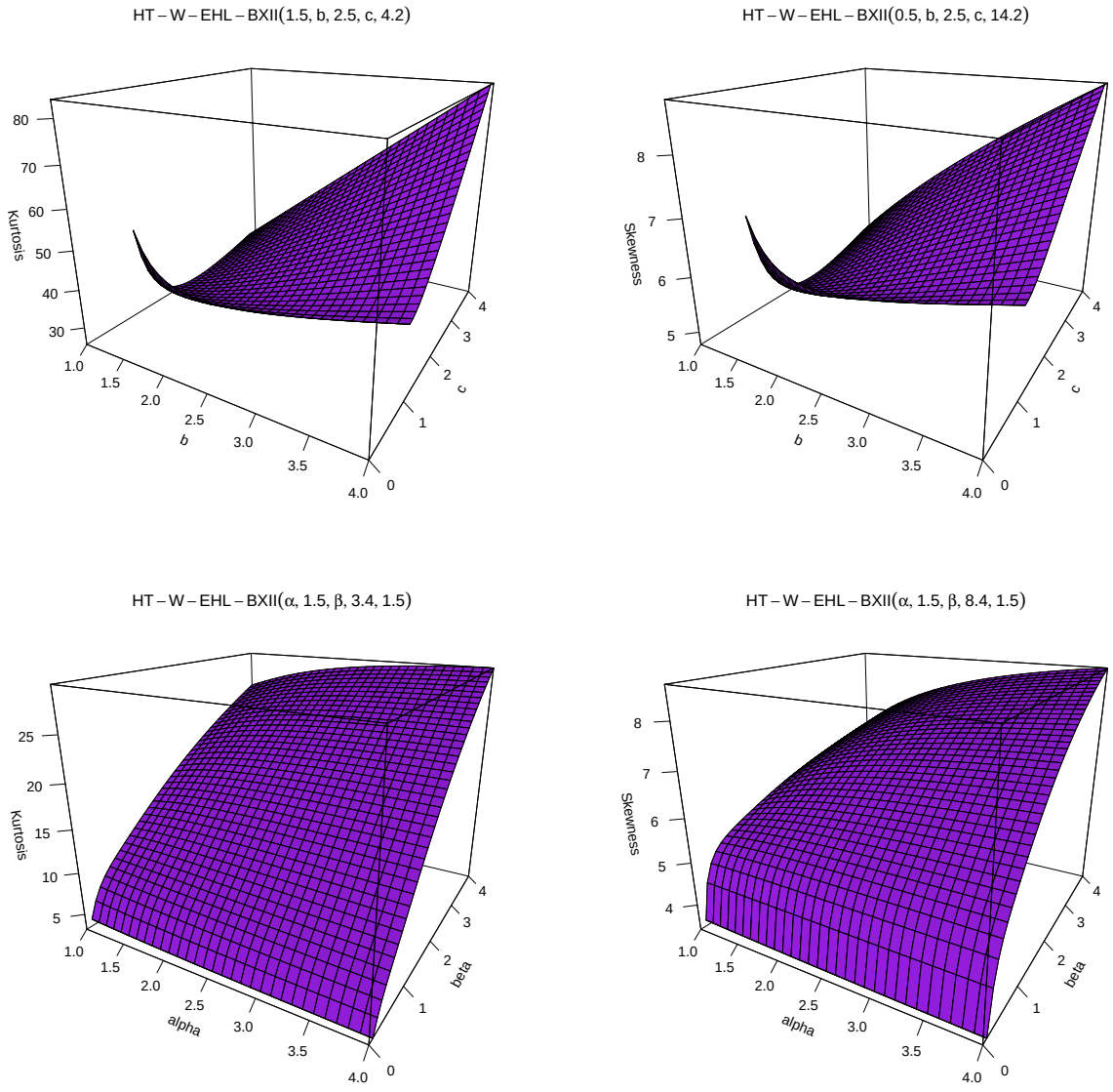

Figure 6. Kurtosis and skewness plots for the HT-W-EHL-BXII distribution

3.1. Quantile function and some distributional characteristics

The QF, defined as the inverse cdf, serves as a fundamental tool for statistical analysis, enabling: (i) random variate generation, (ii) percentile calculation, and (iii) quantile regression among other applications. For the HT-W-EHL-G FoD, we derive the quantile function including specific cases for quartiles and median.

Given the cdf of the HT-W-EHL-G FoD distribution:

$$F(z;\alpha,\beta,\theta,\Upsilon) = 1 - \left(\frac{\exp\left(-\left[-\log\left(1 - \left(\frac{G(z;\Upsilon)}{1+\bar{G}(z;\Upsilon)} \right)^{\alpha} \right) \right]^{\beta} \right)}{1-(1-\theta)\left[1 - \exp\left(-\left[-\log\left(1 - \left(\frac{G(z;\Upsilon)}{1+\bar{G}(z;\Upsilon)} \right)^{\alpha} \right) \right]^{\beta} \right) \right]} \right)^{\theta},$$

we derive the quantile function $Q(p) = F^{-1}(p)$ by setting $F(z;\alpha,\beta,\theta,\Upsilon) = p$, where $p \sim U(0,1)$, that is,

$$p = 1 - \left(\frac{\exp\left(- \left[- \log\left(1 - \left(\frac{G(z;\Upsilon)}{1+\bar{G}(z;\Upsilon)} \right)^{\alpha} \right) \right]^{\beta} \right)}{1 - (1-\theta)\left[1 - \exp\left(- \left[- \log\left(1 - \left(\frac{G(z;\Upsilon)}{1+\bar{G}(z;\Upsilon)} \right)^{\alpha} \right) \right]^{\beta} \right) \right]} \right)^{\theta}.$$

Consequently, the quantile function for the HT-W-EHL-G FoD distribution is

$$Q_p = G^{-1}\left(\frac{2\left[1 - \exp\left(- \left(- \log\left(\frac{\theta(1-p)^{1/\theta}}{1-(1-\theta)(1-p)^{1/\theta}} \right) \right)^{1/\beta} \right) \right]^{1/\alpha}}{1 + \left[1 - \exp\left(- \left(- \log\left(\frac{\theta(1-p)^{1/\theta}}{1-(1-\theta)(1-p)^{1/\theta}} \right) \right)^{1/\beta} \right) \right]^{1/\alpha}} \right), \tag{8}$$

where $G^{-1}(\cdot)$ represents the QF of the baseline distribution.

The quantile function exists when the parent distribution $G(.)$ is well-defined. This allows generating random variates by setting the value p. The quantile function permits direct calculation of key distributional characteristics: the lower quartile ($Q_{0.25}$, 25^{th} percentile), the median ($Q_{0.5}$, 50^{th} percentile) and the upper quartile ($Q_{0.75}$, 75^{th} percentile). Visit the **appendix** for detailed derivations.

3.2. Density expansion

The pdf of the HT-W-EHL-G FoD can be represented as

$$f(z;\alpha,\beta,\theta,\Upsilon) = \sum_{h=0}^{\infty} \Omega_{h+1} g_{h+1}(z;\Upsilon),$$

where $g_{h+1}(z;\Upsilon) = (h+1)g(z;\Upsilon)G^{h}(z;\Upsilon)$ is the exponentiated-G (Expo-G) distribution with power parameter (h+1) and

$$\begin{aligned} \Omega_{h+1} &= 2\alpha\beta\theta^2 \sum_{e,t,r,y,m,u,w=0}^{\infty} \frac{(-1)^{t+v+w+h}[-(t+\theta)]^r}{(h+1)r!} \frac{\Gamma(u+1)}{\Gamma(1)u!} b_{y,m}(1-\theta)^e \binom{\theta+e}{e}\binom{e}{t}\binom{\beta(r+1)-1}{m} \\ &\times \binom{\alpha(\beta(r+1)+y+m+u)-1}{v}\binom{\alpha(\beta(r+1)+y+m+u)+w}{w}\binom{w+v}{h}, \end{aligned} \tag{9}$$

is the linear component. The HT-WEHL-G distribution can be expressed as an infinite linear combination of exponentiated-G (Expo-G) densities, enabling direct derivation of its statistical properties from this linear combination. This representation provides a powerful framework for obtaining the distribution's characteristics, with complete mathematical details available in the appendix.

3.3. Moments and incomplete moments

Moments including the mean, variance, skewness, and kurtosis quantify a distribution's central tendency, dispersion, asymmetry, and tail behavior, respectively. They are also useful in parameter estimation, hypothesis testing, and comparative analysis across distributions in fields like engineering and physics. Let $f(z;\alpha,\beta,\theta,\Upsilon)$ be denoted by $f(z)$.

Suppose W_{m+1} represents an Expo-G distributed random variable with a power parameter $(m+1)$, then the r^{th} moment of the HT-W-EHL-G FoD can be expressed as

$$E\left(Z^r\right) = \int_{-\infty}^{\infty} z^r f(z) dz = \sum_{h=0}^{\infty} \Omega_{h+1} E(W_{h+1}^r),$$

where $E(W_{h+1}^r)$ represents the r^{th} moment of W_{h+1}, and Ω_{h+1} is defined in Equation (9). The r^{th} incomplete moment can be derived as

$$I_Z(t) = \int_0^t z^r f(z)dz = \sum_{h=0}^{\infty} \Omega_{h+1} I_{h+1}(t; r, \Upsilon),$$

where $I_{h+1}(t; r, \Upsilon) = \int_0^t z^r g_{h+1}(z; \Upsilon)dz$ defines the incomplete moment of W_{h+1}. Additionally, the moment generating function (mgf) of Z is

$$M_Z(t) = \sum_{h=0}^{\infty} \Omega_{h+1} E(e^{tW_{h+1}}),$$

with $E(e^{tW_{h+1}})$ representing the mgf of W_{h+1}, and Ω_{h+1} is specified in Equation (9). The derivation of incomplete moments is integral to the formulation of Bonferroni and Lorenz curves, which serve as foundational instruments for examining income disparity, social welfare, and financial risk across diverse disciplines.

3.4. Entropy

Rényi entropy (Rényi [20]) generalizes the concept of Shannon entropy (Shannon [21]) by introducing a tunable parameter to measure uncertainty, diversity, or information content in a system. Widely used in machine learning, ecology, and quantum information, it adapts to contexts requiring weighted emphasis on rare or frequent events.

Rényi entropy for the HT-W-EHL-G FoD is

$$\begin{aligned} I_R(\xi) &= \frac{\log\left[\int_{-\infty}^{\infty} f_{HT-W-EHL-G}^{\xi}(z, \alpha, \beta, \Upsilon)dz\right]}{1-\xi} \\ &= \frac{\log\left[\sum_{t=0}^{\infty} \varphi_t e^{[(1-\xi)I_{REG}]}\right]}{1-\xi}, \xi \neq 1, \xi > 0, \end{aligned} \tag{10}$$

where

$$\begin{aligned} \varphi_t &= \left(\frac{2\alpha\beta\theta^2}{\frac{t}{\xi}+1}\right)^{\xi} \sum_{k,n,p,q,r,s=0}^{\infty} \sum_{m=0}^{k} (-1)^{m+r+s+t+n} \frac{(\theta\xi+m)^n b_{y,p}(1-\theta)^k}{n!(t+1)} \binom{\xi(\theta+1)+k-1}{k} \binom{k}{m} \binom{\xi+q-1}{q} \\ &\times \binom{n\beta+\xi(\beta-1)}{p} \binom{\alpha(n\beta+\xi\beta+p+q+y)-\xi}{r} \binom{\alpha(n\beta+\xi\beta+p+q+y)+\xi+s-1}{s} \binom{r+s}{t} \end{aligned}$$

and $\mathbf{I}_{REG} = \left(\frac{1}{1-\xi}\right) \log\left\{\int_0^{\infty} \left[\left(\frac{t}{\xi}+1\right) g(z; \Upsilon) G^{\frac{t}{\xi}}(z; \Upsilon)\right]^{\xi} dz\right\}$ is the Rényi entropy of the Expo-G distribution with parameter $\left(\frac{t}{\xi}+1\right)$. As a result, Rényi entropy of the HT-W-EHL-G FoD can stem directly from Rényi entropy of the Expo-G distribution. For derivations, visit the appendix.

3.5. Probability weighted moments

Probability weighted moments (PWMs) are less sensitive to outliers than conventional moments, making them ideal for modeling real-world data where extreme events occur like climate extremes, financial crashes, or catastrophic failures. The PWMs for a random variable Z are defined as:

$$M_{p,r,s} = E\left[Z^p (F(Z))^r (1-F(Z))^s\right], \tag{11}$$

where p, r, and s are non-negative integers. For simplicity, we seek to focus on the case where $p = 1$, $r = k$, and $s = 0$, which corresponds to the ordinary PWMs:

$$M_k = E\left[Z(F(Z))^k\right] = \int_{-\infty}^{\infty} z(F(z))^k f(z)dz. \tag{12}$$

After a series of expansions (see appendix) we write

$$M_k = \sum_{v=0}^{\infty} \omega_{v+1} \int_{-\infty}^{\infty} z g_{v+1}(z;\Upsilon)dz, \tag{13}$$

where $g_{v+1}(z;\Upsilon) = (v+1)g(z;\Upsilon)G^v(z;\Upsilon)$ is the Expo-G distribution with power parameter $(v+1)$ and the coefficient ω_{v+1} is given by

$$\begin{aligned}\omega_{v+1} &= 2\alpha\beta\theta^2 \sum_{l,m,p,q,y,s,t,u=0}^{\infty} (-1)^{l+q+t+u+v}(1-\theta)^m b_{y,w} \frac{(p+\theta(l+1))^q}{q!}\binom{k}{l}\binom{\theta(l+1)+m}{m}\binom{m}{p} \\ &\times \binom{\beta(q+1)-1}{w}\binom{\alpha(\beta(q+1)+w+y+s)-1}{t}\binom{\alpha(\beta(q+1)+w+y+s)+u}{u}\binom{u+t}{v}.\end{aligned}$$

Consequently, we can obtain the k^{th} PWM of the HT-W-EHL-G from the moments of the Expo-G FoD. Refer to the appendix for detailed derivations.

4. Estimation Methods

This section implements a multi-faceted estimation framework to determine the parameters of the HT-W-EHL-G distribution. The core methodology employs maximum likelihood (ML) estimation, which is complemented by a suite of alternative techniques including, minimum distance (Anderson-Darling (AD), Right-Tail Anderson-Darling (RTAD)), least squares (ordinary least squares (OLS) and weighted least squares (WLS)), and maximum product of spacings estimators.

4.1. Maximum likelihood estimation

This section presents parameter estimation methods for uncensored and censored datasets via the method of maximum likelihood estimation.

4.1.1. Estimation in the absence of censoring: Given a random sample of size n, where each observation z_i adheres to the HT-W-EHL-G FoD, and considering $\Delta = (\alpha, \beta, \theta, \Upsilon)^T$ as the parameter vector, the log-likelihood function $\ell = \ell(\Delta)$ becomes:

$$\begin{aligned}\ell(\Delta) &= \sum_{i=1}^{n} \log\left(f(z_i;\alpha,\beta,\theta,\Upsilon)\right) \\ &= n\log(2\alpha\beta\theta^2) + \sum_{i=1}^{n}\log\left(g(z_i;\Upsilon)\right) - 2\sum_{i=1}^{n}\log(1+\bar{G}(z_i;\Upsilon)) + (\beta-1)\sum_{i=1}^{n}\log\left(u_i\right) \\ &- \sum_{i=1}^{n}\log(1-v_i^{\alpha}) - \theta\sum_{i=1}^{n}u_i^{\beta} + (\alpha-1)\sum_{i=1}^{n}(\log v_i) - (\theta+1)\sum_{i=1}^{n}\log[1-(1-\theta)(1-e^{-u_i^{\beta}})],\end{aligned} \tag{14}$$

where $v_i = \frac{G(z_i;\Upsilon)}{1+\bar{G}(z_i;\Upsilon)}$ and $u_i = -\log(1-v_i^{\alpha})$.

The numerical solution of the nonlinear equations $\left[\frac{\partial \ell}{\partial \alpha}, \frac{\partial \ell}{\partial \beta}, \frac{\partial \ell}{\partial \theta}, \frac{\partial \ell}{\partial \Upsilon_k}\right]^T = \mathbf{0}$ using iterative methods in R for a specific baseline cdf $G(z;\Upsilon)$, yields the MLE estimates of α, β, θ and Υ_k. Visit the appendix for components of the score vector.

4.1.2. Estimation with censored data: In survival analysis, censored observations are common when only partial event information is available. We focus on right-censored data, where the event time X_k (failure time for the k^{th} subject) may exceed the observation window Y_k (censoring time). For a study with n subjects, we observe (T_k, ϵ_k), where:

$$\epsilon_k = \mathbb{I}(X_k \leq Y_k) = \begin{cases} 1 & \text{if } X_k \leq Y_k \quad \text{(failure observed)}, \\ 0 & \text{if } X_k > Y_k \quad \text{(censored observation)}. \end{cases}$$

Assuming X_k and Y_k are independent and follow the HT-W-EHL-G FoD, the log-likelihood function is:

$$\ell = \sum_{k=1}^{n} \left[\epsilon_k \log f(t_k) + (1-\epsilon_k) \log S(t_k)\right], \tag{15}$$

where $f(\cdot)$ is the pdf and $S(\cdot) = 1 - F(\cdot)$ is the survival function. The MLEs are obtained by numerically optimizing Equation (15)

4.2. Minimum Distance Methods

The underlying principles of the minimum distance estimation methods are to find the parameter estimates that result in the best fit between the estimated cdf and the observed empirical distribution function. This is achieved by minimizing a selected goodness-of-fit statistic, which quantifies the discrepancy between the two distributions. In this subsection, we shall consider two such techniques that are AD and RTAD.

4.2.1. AD and RTAD Methods The AD and RTAD estimates of the HT-W-EHL-G FoDs vector of parameters are respectively found by minimizing the functions:

$$AD(\Delta) = -n - \frac{1}{n}\sum_{i=1}^{n}(2i-1)\left[\log\left(F(z_{(i)}|\alpha,\beta,\theta,\Upsilon)\right) + \log(S(z_{(i)}|\alpha,\beta,\theta,\Upsilon)\right],$$

and

$$RTAD(\Delta) = \frac{n}{2} - 2\sum_{i=1}^{n} F(z_{(i)};\alpha,\beta,\theta,\Upsilon) - \frac{1}{n}\sum_{i=1}^{n}(2i-1)\log S(z_{(n-i+1)};\alpha,\beta,\theta,\Upsilon)$$

with respect to α, β, θ, and Υ, respectively, where $F(.)$ is defined by Equation (4) and $S(.) = 1 - F(.)$.

4.3. Least Squares Methods

Least squares methods determine parameter values by minimizing the sum of squared differences between observed data and the values predicted by the model. Unlike minimum distance methods that focus on distributional fit, least squares often targets direct agreement between empirical and theoretical quantities (such as moments, quantiles, or probabilities). Common variants include ordinary least squares (OLS) and weighted least squares (WLS).

Let $z_{1:n} \leq z_{2:n} \leq z_{3:n} \ldots \leq z_{n:n}$ be order statistics of a random sample of size n drawn from the HT-W-EHL-G FoD. The OLS and WLS estimates of the HT-W-EHL-G FoD vector of parameters are respectively found by minimizing the following functions:

$$OLS(\Delta) \quad = \sum_{i=1}^{n}\left(F(z_{(i)}|\alpha,\beta,\theta,\Upsilon) - \tfrac{i}{n+1}\right)^2,$$

and

$$WLS(\Delta) \quad = \sum_{i=1}^{n}\tfrac{(n+1)^2(n+2)}{i(n-i+1)}\left(F(z_{(i)}|\alpha,\beta,\theta,\Upsilon) - \tfrac{i}{n+1}\right)^2.$$

with respect to $\alpha, \beta, \theta, \Upsilon$.

4.4. MPS Method

The MPS method proposed by Cheng and Amin ([6], [7]), serves as an alternative to the traditional ML estimation approach. Their research showcased that the MPS estimates exhibit favorable statistical characteristics, demonstrating efficiency comparable to maximum likelihood estimates. Within the framework of the HT-W-EHL-G FoD, the MPS parameter vector is determined by maximizing the function

$$MPS(\Delta) \quad = \frac{1}{n+1}\sum_{i=1}^{n+1}\log\left[F(z_{(i)};(\alpha,\beta,\theta,\Upsilon)) - F(z_{(i-1)};(\alpha,\beta,\theta,\Upsilon))\right],$$

with respect to $\alpha, \beta, \theta, \Upsilon$.

5. Simulations

This section examines the consistency of the six parameter estimation techniques through Monte Carlo simulations conducted on the HT-W-EHL-W distribution. The ML, AD, RTAD, OLS, WLS and MPS are the considered estimation techniques. Tables [2] and [3] show the average bias (AvBIAS) and the root mean square error (RMSE) for each estimation technique for various parameter values. The AvBIAS and RMSE for an estimated parameter, for instance ($\hat{\beta}$), are calculated as follows:
AvBIAS($\hat{\beta}$) = $\frac{\sum_{i=1}^{N}\hat{\beta}_i}{N}$ - β and, RMSE($\hat{\beta}$) = $\sqrt{\frac{\sum_{i=1}^{N}(\hat{\beta}_i-\beta)^2}{N}}$, respectively.
Three thousand (N = 3000) replications with sample sizes $n = 20, 50, 100, 300$, and 900, and initial parameter values $(\alpha, b, \beta, d) = (0.4, 0.4, 0.3, 1.5)$ and
$(\alpha, \beta, \theta, d) = (0.2, 1.2, 1.0, 1.2)$ were utilized in the simulation experiments.

Table 2. Simulations results for the various estimation methods with parameter values $\alpha = 0.4, \beta = 0.4, \theta = 0.3, d = 1.5$

		ML		AD		RTAD		OLS		WLS		MPS	
n	Parameters	RMSE	AvBIAS	RMSE	AvBIAS	RMSE	AvBIAS	RMSE	AvBIAS	RMSE	AvBIAS	RMSE	AvBIAS
20	α	$1.0204_{(2)}$	$0.5046_{(2)}$	$1.1982_{(3)}$	$0.5692_{(4)}$	$1.0092_{(1)}$	$0.4903_{(1)}$	$1.3041_{(6)}$	$0.6592_{(6)}$	$1.2376_{(4)}$	$0.5903_{(5)}$	$1.0304_{(5)}$	$0.5384_{(3)}$
	β	$1.3779_{(1)}$	$0.8414_{(1)}$	$1.6321_{(6)}$	$0.9426_{(6)}$	$1.3821_{(2)}$	$0.8429_{(2)}$	$1.4213_{(5)}$	$0.8865_{(4)}$	$1.3863_{(3)}$	$0.8635_{(3)}$	$1.4025_{(4)}$	$0.9213_{(5)}$
	θ	$0.9508_{(1)}$	$0.4717_{(1)}$	$0.9641_{(3)}$	$0.4812_{(2)}$	$0.9621_{(2)}$	$0.4821_{(3)}$	$0.9743_{(5)}$	$0.4832_{(4)}$	$0.9923_{(6)}$	$0.4977_{(6)}$	$0.9734_{(4)}$	$0.4876_{(5)}$
	d	$1.2938_{(2)}$	$0.4199_{(2)}$	$1.3021_{(4)}$	$0.4291_{(4)}$	$1.1993_{(1)}$	$0.3921_{(1)}$	$1.3512_{(6)}$	$0.5314_{(6)}$	$1.3217_{(5)}$	$0.5143_{(5)}$	$1.2957_{(3)}$	$0.4201_{(3)}$
	$\sum$ ranks		12		32		15		42		37		32
50	α	$0.8551_{(2)}$	$0.3591_{(3)}$	$0.9929_{(6)}$	$0.3498_{(1)}$	$0.9034_{(4)}$	$0.5238_{(4)}$	$0.9074_{(4)}$	$0.4032_{(5)}$	$0.8532_{(1)}$	$0.3542_{(2)}$	$0.9355_{(5)}$	$0.4127_{(6)}$
	β	$1.0189_{(2)}$	$0.5342_{(1)}$	$1.2146_{(5)}$	$0.6389_{(5)}$	$1.0231_{(3)}$	$0.5441_{(2)}$	$1.2367_{(6)}$	$0.5539_{(3)}$	$1.0155_{(1)}$	$0.6001_{(4)}$	$1.2034_{(4)}$	$0.7269_{(6)}$
	θ	$0.7444_{(1)}$	$0.3058_{(1)}$	$0.7526_{(2)}$	$0.3102_{(2)}$	$0.7621_{(3)}$	$0.3103_{(3)}$	$0.8058_{(5)}$	$0.4112_{(5)}$	$0.9032_{(6)}$	$0.5326_{(6)}$	$0.7638_{(4)}$	$0.3126_{(4)}$
	d	$1.1921_{(2)}$	$0.3796_{(1)}$	$1.2221_{(4)}$	$0.3841_{(2)}$	$1.1865_{(1)}$	$0.3921_{(3)}$	$1.2731_{(6)}$	$0.4136_{(5)}$	$1.2608_{(5)}$	$0.4241_{(6)}$	$1.1938_{(3)}$	$0.4013_{(4)}$
	$\sum$ ranks		13		27		22		39		31		36
100	α	$0.6128_{(1)}$	$0.1914_{(1)}$	$0.7321_{(4)}$	$0.2141_{(5)}$	$0.6213_{(2)}$	$0.1983_{(2)}$	$0.7412_{(5)}$	$0.2113_{(4)}$	$0.6849_{(3)}$	$0.2003_{(3)}$	$0.8217_{(6)}$	$0.2264_{(6)}$
	β	$0.7593_{(1)}$	$0.2782_{(1)}$	$0.8469_{(6)}$	$0.3431_{(6)}$	$0.7921_{(2)}$	$0.2843_{(2)}$	$0.8416_{(5)}$	$0.3421_{(5)}$	$0.8026_{(3)}$	$0.2863_{(3)}$	$0.8249_{(4)}$	$0.3216_{(4)}$
	θ	$0.5357_{(1)}$	$0.1654_{(1)}$	$0.5426_{(3)}$	$0.1728_{(4)}$	$0.5462_{(5)}$	$0.1799_{(5)}$	$0.5429_{(4)}$	$0.1721_{(3)}$	$0.5945_{(6)}$	$0.1811_{(6)}$	$0.5421_{(2)}$	$0.1719_{(2)}$
	d	$1.0641_{(3)}$	$0.2005_{(3)}$	$1.0763_{(6)}$	$0.2114_{(4.5)}$	$1.0746_{(5)}$	$0.2147_{(6)}$	$1.0763_{(4)}$	$0.2114_{(4.5)}$	$1.0635_{(2)}$	$0.2003_{(2)}$	$0.9923_{(1)}$	$0.1992_{(1)}$
	$\sum$ ranks		12		38.5		29		34.5		32		26
300	α	$0.2229_{(2)}$	$0.0381_{(3)}$	$0.3260_{(6)}$	$0.0458_{(6)}$	$0.2341_{(4)}$	$0.0421_{(5)}$	$0.2243_{(3)}$	$0.0364_{(2)}$	$0.2148_{(1)}$	$0.0321_{(1)}$	$0.2514_{(5)}$	$0.0403_{(4)}$
	β	$0.5460_{(3)}$	$0.1256_{(3)}$	$0.5341_{(1)}$	$0.1162_{(1)}$	$0.5490_{(4)}$	$0.1286_{(4)}$	$0.5926_{(5)}$	$0.1368_{(5)}$	$0.5392_{(2)}$	$0.1212_{(2)}$	$0.6239_{(6)}$	$0.1423_{(6)}$
	θ	$0.2887_{(1)}$	$0.0462_{(1)}$	$0.3221_{(4)}$	$0.0501_{(3)}$	$0.2931_{(2)}$	$0.0521_{(3)}$	$0.3141_{(3)}$	$0.0593_{(4)}$	$0.3247_{(5)}$	$0.0731_{(6)}$	$0.3296_{(6)}$	$0.0632_{(5)}$
	d	$0.7830_{(1)}$	$0.1152_{(1)}$	$0.7923_{(3)}$	$0.1205_{(3)}$	$0.7926_{(4)}$	$0.1237_{(4)}$	$0.8219_{(6)}$	$0.1314_{(6)}$	$0.7859_{(2)}$	$0.1187_{(2)}$	$0.7930_{(5)}$	$0.1246_{(5)}$
	$\sum$ ranks		15		27		30		34		21		42
900	α	$0.1775_{(3)}$	$0.0154_{(3)}$	$0.1821_{(5)}$	$0.0213_{(6)}$	$0.1628_{(1)}$	$0.0142_{(1.5)}$	$0.1699_{(2)}$	$0.0142_{(1.5)}$	$0.1782_{(4)}$	$0.0169_{(4)}$	$0.1824_{(6)}$	$0.0175_{(5)}$
	β	$0.3156_{(2)}$	$0.0391_{(2)}$	$0.2993_{(1)}$	$0.0316_{(1)}$	$0.3421_{(5.5)}$	$0.0469_{(5.5)}$	$0.3292_{(4)}$	$0.0415_{(4)}$	$0.3184_{(3)}$	$0.0401_{(3)}$	$0.3421_{(5.5)}$	$0.0469_{(5.5)}$
	θ	$0.1477_{(1)}$	$0.0104_{(2)}$	$0.1463_{(1)}$	$0.0109_{(3)}$	$0.1521_{(3)}$	$0.0164_{(5)}$	$0.1491_{(5)}$	$0.0116_{(2)}$	$0.1503_{(2)}$	$0.0142_{(4)}$	$0.1739_{(6)}$	$0.0341_{(6)}$
	d	$0.0530_{(2)}$	$0.0141_{(2)}$	$0.0821_{(6)}$	$0.0186_{(6)}$	$0.0631_{(5)}$	$0.0158_{(4)}$	$0.0598_{(3)}$	$0.0162_{(5)}$	$0.0305_{(1)}$	$0.0095_{(1)}$	$0.0613_{(4)}$	$0.0151_{(3)}$
	$\sum$ ranks		17		29		30.5		26.5		22		41

Tables [2] and [3] include a row labeled '$\sum$ ranks' which represents the partial sum of the ranks. The subscript (in parenthesis) next to each estimate indicates its rank for a specific metric. For instance, in Table [3], the RMSE of $\hat{\beta}$ obtained through the RTAD method is shown as $1.9024_{(6)}$ for $n = 20$. This means that the RTAD method ranks sixth among other estimators in terms of RMSE of $\hat{\beta}$. Furthermore, the AvBIAS of $\hat{\alpha}$ derived by the ML approach is $0.2946_{(1)}$ for $n = 50$, signifying the best AvBIAS of $\hat{\alpha}$ when compared to other estimates. Table [4]

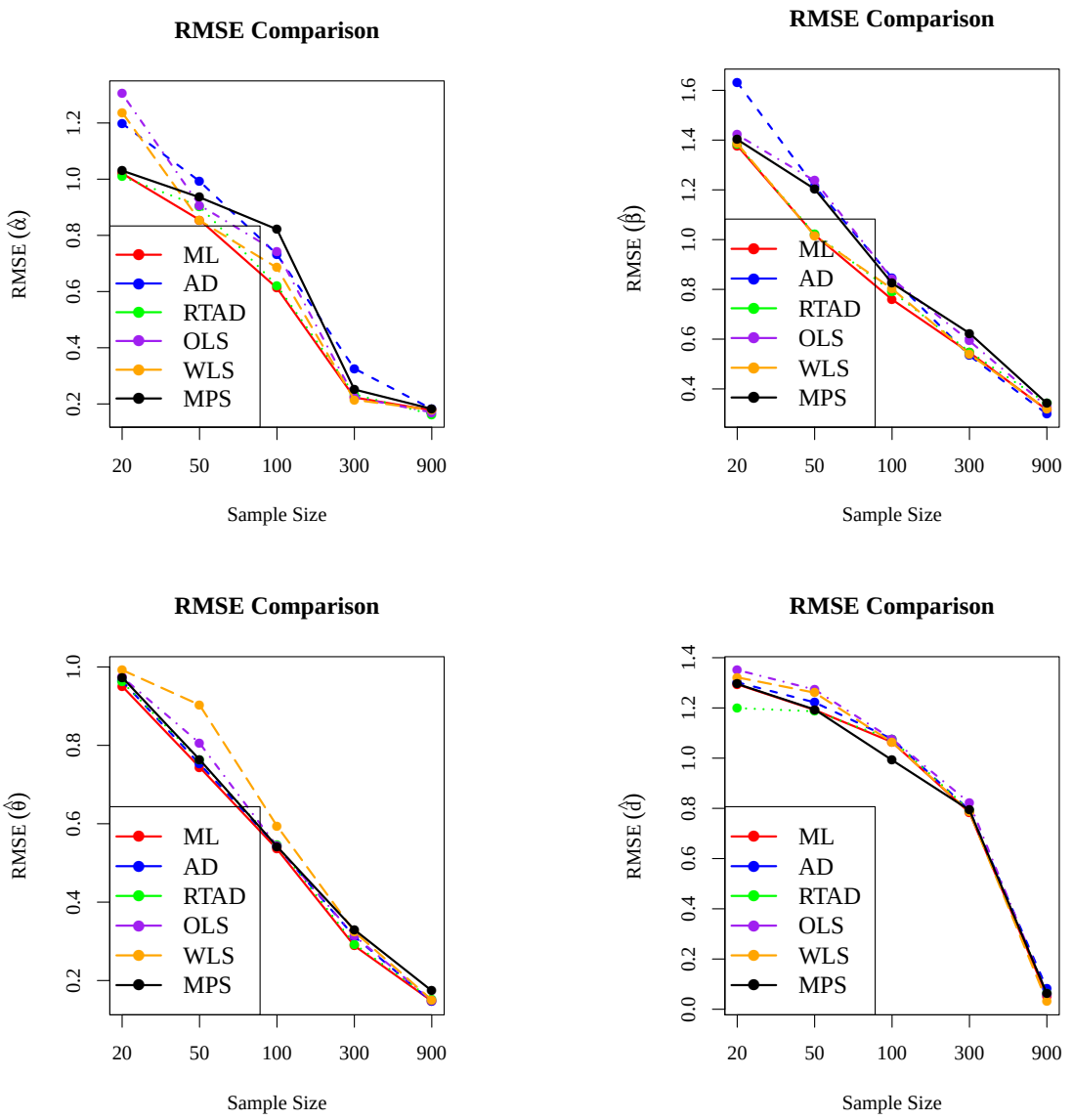

Figure 7. Plots illustrating the reduction in RMSEs for parameter values ($\alpha = 0.4, b = 0.4, \beta = 0.3,$ and $d = 1.5$) with increasing sample size

presents the partial and final ranks assigned to the estimation techniques employed in estimating the HT-W-EHL-W distribution across different model parameter values. Figures [7] and [8] show line plots depicting the gradual decrease in RMSEs for the estimated parameters with increasing sample size for each of the estimation methods. Based on the findings presented in Tables [2] and [3], the following conclusions can be drawn:

- HT-W-EHL-W distribution exhibited stability, as indicated by the modest values of AVBIAS and RMSE for its four parameters.
- RMSE and AvBIAS consistently decreased with increasing sample size across all estimating methods.
- Reliable estimations were achieved across all estimation methods, particularly when larger sample sizes were employed.

Table 3. Simulations results for the various estimation methods with parameter values $\alpha = 0.2, \beta = 1.2, \theta = 1.0, d = 1.2$

		ML		AD		RTAD		OLS		WLS		MPS	
n	Parameters	RMSE	AvBIAS	RMSE	AvBIAS	RMSE	AvBIAS	RMSE	AvBIAS	RMSE	AvBIAS	RMSE	AvBIAS
20	α	$0.9220_{(2)}$	$0.4354_{(2)}$	$1.0272_{(4)}$	$0.4632_{(3)}$	$0.9784_{(3)}$	$0.5592_{(5)}$	$1.3412_{(5)}$	$0.5234_{(4)}$	$0.8922_{(1)}$	$0.4233_{(1)}$	$2.0103_{(6)}$	$0.9592_{(6)}$
	β	$1.9637_{(6)}$	$0.5890_{(6)}$	$1.9402_{(5)}$	$0.5793_{(5)}$	$1.9321_{(4)}$	$0.5428_{(3)}$	$1.9235_{(3)}$	$0.5346_{(2)}$	$1.0358_{(1)}$	$0.4401_{(1)}$	$1.8752_{(2)}$	$0.5764_{(4)}$
	θ	$1.8843_{(4)}$	$0.9361_{(4)}$	$1.8824_{(3)}$	$0.9324_{(3)}$	$1.9024_{(6)}$	$0.9436_{(6)}$	$1.8521_{(1)}$	$0.8921_{(1)}$	$1.8621_{(2)}$	$0.9021_{(2)}$	$1.9004_{(5)}$	$0.9421_{(5)}$
	d	$0.8988_{(2)}$	$0.1094_{(2)}$	$0.9001_{(3)}$	$0.1104_{(3)}$	$0.9104_{(4)}$	$0.1184_{(4)}$	$0.9121_{(5)}$	$0.1196_{(5)}$	$0.8841_{(1)}$	$0.0934_{(1)}$	$0.9126_{(6)}$	$0.1199_{(6)}$
	$\sum$ ranks		28		29		35		26		10		40
50	α	$0.6477_{(1)}$	$0.2946_{(1)}$	$0.7506_{(3)}$	$0.3686_{(3)}$	$0.7632_{(4)}$	$0.3808_{(5)}$	$0.7721_{(5)}$	$0.3721_{(4)}$	$0.6521_{(2)}$	$0.3051_{(2)}$	$1.5249_{(6)}$	$0.6359_{(6)}$
	β	$1.7675_{(2)}$	$0.4700_{(2)}$	$1.8346_{(6)}$	$0.4836_{(6)}$	$1.8299_{(4.5)}$	$0.4803_{(4.5)}$	$1.8299_{(4.5)}$	$0.4803_{(4.5)}$	$0.9947_{(1)}$	$0.3924_{(1)}$	$1.7734_{(3)}$	$0.4726_{(3)}$
	θ	$1.1580_{(2)}$	$0.4728_{(2)}$	$1.1603_{(3)}$	$0.4828_{(3)}$	$1.1704_{(5)}$	$0.4903_{(5)}$	$1.1621_{(4)}$	$1.4828_{(4)}$	$1.1821_{(6)}$	$0.5121_{(6)}$	$1.1528_{(1)}$	$0.4704_{(1)}$
	d	$0.7709_{(1)}$	$0.1004_{(1)}$	$0.7923_{(2.5)}$	$0.1099_{(2.5)}$	$0.8034_{(5)}$	$0.1103_{(5)}$	$0.7923_{(2.5)}$	$0.1099_{(2.5)}$	$0.7834_{(4)}$	$0.1027_{(4)}$	$0.8155_{(6)}$	$0.1128_{(6)}$
	$\sum$ ranks		12		29		37		32		26		32
100	α	$0.4985_{(2)}$	$0.1919_{(2)}$	$0.5331_{(4)}$	$0.2141_{(4)}$	$0.6121_{(5)}$	$0.2697_{(5)}$	$0.4921_{(1)}$	$0.1901_{(1)}$	$0.5037_{(3)}$	$0.2001_{(3)}$	$1.0249_{(6)}$	$0.4359_{(6)}$
	β	$1.6197_{(3)}$	$0.3293_{(3)}$	$1.6265_{(4)}$	$0.3301_{(4)}$	$1.6137_{(2)}$	$0.3258_{(2)}$	$1.6401_{(5)}$	$0.3421_{(5)}$	$0.8921_{(1)}$	$0.1427_{(1)}$	$1.6454_{(6)}$	$0.3468_{(6)}$
	θ	$0.8190_{(2)}$	$0.1129_{(2)}$	$0.8055_{(1)}$	$0.1101_{(1)}$	$0.8203_{(3)}$	$0.1203_{(3)}$	$0.8235_{(4)}$	$0.1248_{(4)}$	$0.8941_{(6)}$	$0.1428_{(6)}$	$0.8331_{(5)}$	$0.1369_{(5)}$
	d	$0.6442_{(1)}$	$0.0900_{(1)}$	$0.6623_{(4)}$	$0.0997_{(4)}$	$0.6587_{(3)}$	$0.0921_{(3)}$	$0.6625_{(5)}$	$0.0998_{(5)}$	$0.6536_{(2)}$	$0.0901_{(2)}$	$0.6664_{(6)}$	$0.1053_{(6)}$
	$\sum$ ranks		16		26		26		30		24		46
300	α	$0.2510_{(1)}$	$0.0669_{(1)}$	$0.2739_{(4)}$	$0.0835_{(4)}$	$0.3604_{(5)}$	$0.1336_{(5)}$	$0.2642_{(3)}$	$0.0800_{(3)}$	$0.2633_{(2)}$	$0.0742_{(2)}$	$0.8516_{(6)}$	$0.2539_{(6)}$
	β	$0.3400_{(1)}$	$0.2470_{(1)}$	$0.3427_{(3)}$	$0.2481_{(3)}$	$0.3401_{(2)}$	$0.2392_{(2)}$	$0.3465_{(4)}$	$0.2501_{(4)}$	$0.3907_{(6)}$	$0.2713_{(6)}$	$0.3651_{(5)}$	$0.2603_{(5)}$
	θ	$0.6343_{(4)}$	$0.0322_{(4)}$	$0.6421_{(5)}$	$0.0395_{(5)}$	$0.6321_{(3)}$	$0.0299_{(3)}$	$0.6246_{(2)}$	$0.0214_{(4)}$	$0.6121_{(1)}$	$0.0123_{(1)}$	$0.6467_{(6)}$	$0.0401_{(6)}$
	d	$0.2789_{(1)}$	$0.0437_{(1)}$	$0.3022_{(5)}$	$0.0654_{(5)}$	$0.2994_{(4)}$	$0.0536_{(4)}$	$0.2801_{(2)}$	$0.0502_{(2)}$	$0.2831_{(3)}$	$0.0504_{(3)}$	$0.3155_{(6)}$	$0.0651_{(6)}$
	$\sum$ ranks		17		34		28		22		24		46
900	α	$0.1227_{(2)}$	$0.0184_{(2)}$	$0.1321_{(4)}$	$0.0211_{(4)}$	$0.1383_{(5)}$	$0.0436_{(5)}$	$0.1299_{(3)}$	$0.0201_{(3)}$	$0.1164_{(1)}$	$0.0106_{(1)}$	$0.1986_{(6)}$	$0.1067_{(6)}$
	β	$0.0697_{(4)}$	$0.0505_{(4)}$	$0.0583_{(3)}$	$0.0491_{(3)}$	$0.0428_{(2)}$	$0.0427_{(2)}$	$0.0736_{(5)}$	$0.0525_{(5)}$	$0.0401_{(1)}$	$0.0321_{(1)}$	$0.0816_{(6)}$	$0.0699_{(6)}$
	θ	$0.3146_{(4)}$	$0.0293_{(4)}$	$0.3293_{(6)}$	$0.0311_{(6)}$	$0.3027_{(2)}$	$0.0212_{(2)}$	$0.3114_{(3)}$	$0.0263_{(3)}$	$0.2934_{(1)}$	$0.0143_{(1)}$	$0.3251_{(5)}$	$0.0304_{(5)}$
	d	$0.0087_{(1)}$	$0.0140_{(1)}$	$0.0115_{(5)}$	$0.0199_{(5)}$	$0.0106_{(4)}$	$0.0187_{(4)}$	$0.0103_{(2.5)}$	$0.0184_{(2.5)}$	$0.0103_{(2.5)}$	$0.0157_{(2.5)}$	$0.0205_{(6)}$	$0.0231_{(6)}$
	$\sum$ ranks		22		36		26		26		11		46

Table 4. Rankings of estimation methods for HT-W-EHL-W distribution across different values of the model parameters

Parameters	n	ML	AD	RTAD	OLS	WLS	MPS
$\alpha = 0.4, \beta = 0.4, \theta = 0.3, d = 1.5$	20	1	3.5	2	6	5	3.5
	40	1	3	2	6	4	5
	100	1	6	3	5	4	2
	300	1	3	4	5	2	6
	900	1	4	5	2	3	6
$\alpha = 0.2, \beta = 1.2, \theta = 1.0, d = 1.2$	20	4	3	5	2	1	6
	40	1	3	6	4.5	2	4.5
	100	1	3.5	3.5	5	2	6
	300	1	5	4	2	3	6
	900	2	5	3.5	3.5	1	6
	$\sum$ ranks	14	39	38	41	27	51
	Final ranking	1	4	3	5	2	6

Table [4] demonstrates that the ML emerged as the most effective technique in providing accurate estimates for the HT-W-EHL-W distribution parameters. Consequently, we proceeded to estimate the HT-W-EHL-W distribution's unknown parameters.

6. Risk Measures

Risk measures are fundamental quantitative tools in actuarial science and financial mathematics for assessing and managing exposure to extreme events. In this section, we examine four key risk metrics for the HT-W-EHL-G FoD:

(i) Value at risk (VaR): The minimum potential loss at a specified confidence level p, defined as:

$$\text{VaR}_p = F^{-1}(p), \tag{16}$$

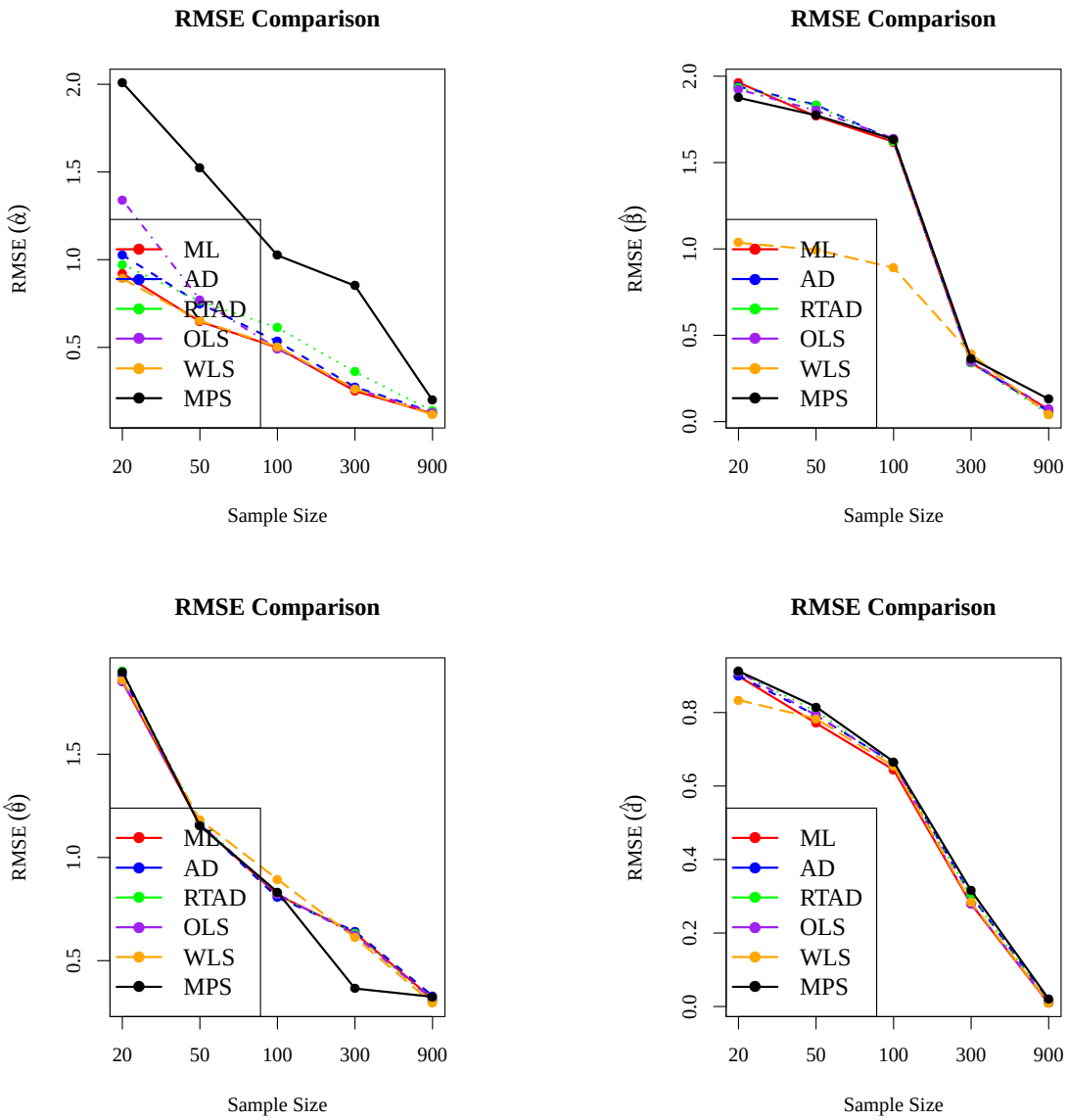

Figure 8. Plots depicting reduction in RMSEs for parameter values ($\alpha = 0.2, \beta = 1.2, \theta = 1.0, d = 1.2$) with increasing sample size

where $F^{-1}(\cdot)$ is the QF of the distribution and $p \in (0,1)$ is the probability level. Consequently, for the HT-W-EHL-G FoD, we compute VaR_p as

$$VaR_p = G^{-1}\left(\frac{2\left[1-\exp\left(-\left(-\log\left(\frac{\theta(1-p)^{1/\theta}}{1-(1-\theta)(1-p)^{1/\theta}}\right)\right)^{1/\beta}\right)\right]^{1/\alpha}}{1+\left[1-\exp\left(-\left(-\log\left(\frac{\theta(1-p)^{1/\theta}}{1-(1-\theta)(1-p)^{1/\theta}}\right)\right)^{1/\beta}\right)\right]^{1/\alpha}}\right). \tag{17}$$

(ii) Tail value at visk (TVaR): The expected conditional loss not exceeding the VaR threshold expressed as

$$\text{TVaR}_p = \frac{1}{1-p}\int_{VaR_p}^{\infty} zf(z)dz. \tag{18}$$

Therefore, TVaR for HT-W-EHL-G FoD is

$$TVaR_p = \frac{1}{1-p}\sum_{h=0}^{\infty}\int_{VaR_p}^{\infty} z\Omega_{h+1}g_{h+1}(z;\Upsilon)dz, \tag{19}$$

where Ω_{h+1} is defined as stated in Equation (9) and $g_{h+1}(z;\Upsilon) = (h+1)G^h(z;\Upsilon)g(z;\Upsilon)$ represents the Expo-G pdf with a power parameter $(h+1)$.

(iii) Tail variance (TV): Measures dispersion of losses beyond the VaR threshold. TV is given by

$$TV_p = E\left(Z^2 \mid Z > z_p\right) - \left(TVaR_p\right)^2. \tag{20}$$

The TV of the HT-W-EHL-G FoD is

$$\begin{aligned} TV_p &= \frac{1}{1-p}\int_{VaR_p}^{\infty} z^2 f(z)dz - \left(TVaR_p\right)^2 \\ &= \frac{1}{1-p}\sum_{h=0}^{\infty}\Omega_{h+1}\int_{VaR_p}^{\infty} z^2 g_{h+1}(z;\Upsilon)dz - \left(TVaR_p\right)^2, \end{aligned} \tag{21}$$

where $g_{h+1}(z;\Upsilon) = (h+1)G^h(z;\Upsilon)g(z;\Upsilon)$ is the Expo-G distribution with power parameter $(h+1)$. The vector Υ represents the parameters of the parent distribution, while Ω_{h+1} is given in Equation (9). Hence, the TV_p of HT-W-EHL-G FoD can be obtained from those of Expo-G distributions.

(iv) Tail Variance Premium (TVP): A coherent risk measure that combines the expected loss in the tail (TVaR) with the variability of those losses (TV), scaled by a risk aversion factor:

$$\text{TVP}_p = \text{TVaR}_p + \varphi TV_p \tag{22}$$

where $\varphi > 0$ is a risk aversion parameter.

6.1. Numerical study for the risk measures

We present results from the numerical simulations for the risk measures of the HT-W-EHL-W distribution in this subsection. The risk measures (TVaR, VaR, TV and TVP) of the HT-W-EHL-W distribution are compared to the Weibull-exponentiated half logistic-Weibull (W-EHL-W), type-I-heavy-tailed-Weibull (TI-HT-W), the one-parameter and two-parameter Weibull distributions. Simulation results are obtained based on the following:

(1) Samples of size 100 are randomly generated from each of the specified distributions, and the parameters are estimated using the maximum likelihood method.
(2) The calculations for the risk measures are performed through 1000 repetitions for these distributions.

The risk measures for four heavy-tailed distributions are presented in Table 5. A model with higher values of VaR, TVaR, TV, and TVP is considered to have a more pronounced heavy tail. We can conclude that the HT-W-EHL-W distribution has a heavier tail compared to the W-EHL-W, TIHT-W, and the Weibull distributions. The HT-W-EHL-W distribution is thus best suited to modeling heavy-tailed data due to its higher risk measurements.

7. Applications

This section presents an empirical evaluation of the proposed HT-W-EHL-G model through its HT-W-EHL-W sub-model application. We conduct comparative analysis against competing heavy-tailed distributions, exponentiated half-logistic and Weibull extensions, including:

Table 5. Simulation Results of VaR, TVaR, TV and TVP

		Significance level				
Distribution	Risk measure	0.75	0.8	0.85	0.9	0.95
HT-W-EHL-W($\alpha=1.4,\beta=2.3,\theta=0.52,d=0.9$)	VaR	56.3842	66.6245	71.8969	82.7442	103.5557
	TVaR	90.4654	94.0229	112.7210	115.0567	136.6641
	TV	284.1546	290.4687	296.4358	307.7864	326.7921
	TVP	427.1680	429.7012	486.6385	507.3259	610.4656
W-EHL-W($\alpha=1.4,\beta=2.3,d=0.9$)	VaR	11.6489	13.6245	15.10569	20.7442	23.4747
	TVaR	33.2001	34.4251	37.4785	41.0792	56.2354
	TV	45.1525	64.9657	66.1256	87.0946	96.2467
	TVP	97.1356	107.0987	111.9876	119.3645	145.9776
TI-HT-W($\theta=0.52,d=0.9$)	VaR	1.0254	1.9756	2.3547	3.0021	5.1456
	TVaR	6.1376	6.9356	7.4878	8.902	8.7433
	TV	10.3593	12.3214	13.6543	14.4244	17.2153
	TVP	21.7396	29.1245	31.2432	33.2754	37.7245
Weibull($d=0.9$)	VaR	0.0045	0.0078	0.0178	0.0356	0.2523
	TVaR	0.1253	0.1546	0.1923	0.2577	0.2909
	TV	0.4690	0.5704	0.7797	0.8902	0.9918
	TVP	1.0975	1.5987	1.9765	2.7421	3.9754

(i) The exponentiated half logistic odd Burr III log-logistic (EHL-OBIII-LLoG) (Oluyede et al. [18]) with pdf

$$\begin{aligned} f(x) &= 2\alpha ab\left(\left(1+\left(\frac{1-(1+x^{\lambda})^{-1}}{(1+x^{\lambda})^{-1}}\right)^{-\alpha}\right)^{-b}\right)^{\alpha-1}\left(1+\left(\frac{1-(1+x^{\lambda})^{-1}}{(1+x^{\lambda})^{-1}}\right)^{-\alpha}\right)^{-b-1} \\ &\times \left(1+\left[1-\left(1+\left(\frac{1-(1+x^{\lambda})^{-1}}{(1+x^{\lambda})^{-1}}\right)^{-\alpha}\right)^{-b}\right]\right)^{-(\alpha+1)}\left(\frac{1-(1+x^{\lambda})^{-1}}{(1+x^{\lambda})^{-1}}\right)^{-\alpha-1} \\ &\times \frac{\lambda x^{\lambda-1}(1+x^{\lambda})^{-2}}{\left((1+x^{\lambda})^{-1}\right)^{2}}, \end{aligned}$$

for $\alpha, a, b, \lambda > 0$.

(ii) The gamma type II exponentiated half logistic-Topp-Leone-Weibull (RB-TII-EHL-TL-W) (Charumbira et al. [5]) with pdf

$$\begin{aligned} f(z) &= \frac{4\alpha\vartheta}{\Gamma(\sigma)}\left(-\log\left[1-W_W(z;\alpha,\vartheta,\lambda)\right]\right)^{\sigma-1}\frac{\lambda z^{\lambda-1}\exp(-z^{\lambda})[1-\exp(-2z^{\lambda})]^{\vartheta-1}\exp(-z^{\lambda})}{(1+[1-\exp(-2z^{\lambda})]^{\vartheta})^{\alpha+1}} \\ &\times \left(1-[1-\exp(-2z^{\lambda})]^{\vartheta}\right)^{\alpha-1}, \end{aligned}$$

for $\sigma, \alpha, \vartheta, \lambda > 0$, where $W_W(z;\alpha,\vartheta,\lambda) = \left(\frac{1-[1-\exp(-2z^{\lambda})]^{\vartheta}}{1+[1-\exp(-2z^{\lambda})]^{\vartheta}}\right)^{\alpha}$.

(iii) The odd exponentiated half logistic Burr XII (OEHL-BXII) by Aldahlan and Afify [2] with pdf

$$\begin{aligned} f(w) &= 2\alpha\beta\delta c w^{\delta-1}\exp\left\{\beta\left[1-\left(1+w^{\delta}\right)^{c}\right]\right\}\left(1-\exp\left\{\beta\left[1-\left(1+w^{\delta}\right)^{c}\right]\right\}\right)^{\alpha-1} \\ &\times \left[\left(1+w^{\delta}\right)^{-c+1}\left(1+\exp\left\{\beta\left[1-\left(1+w^{\delta}\right)^{c}\right]\right\}\right)^{\alpha+1}\right]^{-1}, \end{aligned}$$

where α, β, δ, c are positive parameters.

(iv) Kumaraswamy Weibull distribution (KW) by Cordeiro et al. [9] whose pdf is

$$f(x) = ab\alpha^{\beta}x^{\beta-1}\exp\left(-\alpha x^{\beta}\right)\left(1-\exp\left(-\alpha x^{\beta}\right)\right)^{a-1}\left[1-\left(1-\exp-(\alpha x)^{\beta}\right)^{a}\right]^{b-1}$$

for $a, b, \alpha, \beta > 0$ and $x > 0$.

(v) The exponential Lindley odd log-logistic Weibull (ELOLLW) by Korkmaz et al. [12] with pdf

$$f(x) = \frac{\theta^2\gamma\lambda^\gamma x^{\gamma-1}\exp-(\lambda x)^\gamma\left(\exp-(\lambda x)\right)^{\theta-1}\left(1-\exp-(\lambda x)^\gamma\right)^{-1}}{(\theta+\beta)\left[\left(1-\exp-(\lambda x)^\gamma\right)+\exp-(\lambda x)^\gamma\right]^{\theta-1}}\left(1-\beta\log\left[\frac{\exp-(\lambda x)^\gamma}{1-\exp-(\lambda x)^\gamma+\exp-(\lambda x)^\gamma}\right]\right)$$

for $\beta,\lambda,\theta,\gamma>0$ and $x>0$.

(vi) The type I heavy-tailed odd power generalized Weibull-Weibull (TI-HT-OPGW-W) by Moakofi et al. [14] with pdf

$$f(x) = \theta^2\alpha\beta\left[1+(W(x;\lambda))^\alpha\right]^{\beta-1}(W(x;\lambda))^{\alpha-1}\exp\left(\theta\left(1-\left[1+(W(x;\lambda))^\alpha\right]^\beta\right)\right)\frac{\frac{x}{\lambda^2}\exp\left(-\frac{x^2}{2\lambda^2}\right)}{\left(\exp\left(-\frac{x^2}{2\lambda^2}\right)\right)^2}$$
$$\times\left(1-\bar{\theta}\left[1-\exp\left(1-\left[1+(W(x;\lambda))^\alpha\right]^\beta\right)\right]\right)^{-(\theta+1)},$$

where $W(x;\lambda)=\frac{1-\exp\left(-\frac{x^2}{2\lambda^2}\right)}{\exp\left(-\frac{x^2}{2\lambda^2}\right)}$ for $\theta,\alpha,\beta,\lambda>0$ and $\bar{\theta}=1-\theta$.

To evaluate and compare the performance of the competing models, we employ seven goodness-of-fit (GoF) measures: the log-likelihood (-2log(L)), which assesses the model's overall fit to the data; the Akaike Information Criterion (AIC) and Bayesian Information Criterion (BIC), which balance model fit with complexity by penalizing additional parameters; the Consistent Akaike Information Criterion (CAIC), which provides a stricter penalty for overparameterization, Cramér-von Mises (W^*), Anderson-Darling (A^*) and the Kolmogorov-Smirnov (K-S) test statistic along with its associated p-value, which quantifies the maximum distance between the empirical and fitted cdfs.

To estimate the parameters of the HT-W-EHL-W model, the non-linear minimization function (nlm) in R software was utilized. Parameter estimates accompanied by their respective standard errors (SEs), are indicated within parentheses. To verify the identifiability of parameter estimates, profile log-likelihood plots were constructed for all analyzed datasets. The model validation was further supported through multi-faceted graphical diagnostics, including: (i) fitted probability density curves, (ii) probability-probability (P-P) plots, (iii) empirical cumulative distribution functions (ECDFs), (iv) Kaplan-Meier (K-M) survival curves, (v) scaled total time on test (TTT) transformations, and (vi) hrf plots.

7.1. Fracture toughness of alumina data

The first dataset represents the fracture toughness of material Alumina (AI_2O_3) as discussed by Arshad et al. [4]. The values are: 5.5, 5, 4.9, 6.4, 5.1, 5.2, 5.2,5, 4.7, 4, 4.5, 4.2, 4.1, 4.56, 5.01, 4.7, 3.13, 3.12, 2.68, 2.77, 2.7, 2.36, 4.38, 5.73, 4.35, 6.81, 1.91, 2.66, 2.61, 1.68, 2.04, 2.08, 2.13, 3.8, 3.73, 3.71, 3.28, 3.9, 4, 3.8, 4.1, 3.9, 4.05, 4, 3.95, 4, 4.5, 4.5, 4.2, 4.55, 4.65, 4.1, 4.25, 4.3, 4.5, 4.7, 5.15, 4.3, 4.5, 4.9, 5, 5.35, 5.15, 5.25, 5.8, 5.85, 5.9, 5.75, 6.25, 6.05, 5.9, 3.6, 4.1, 4.5, 5.3, 4.85, 5.3, 5.45, 5.1, 5.3, 5.2, 5.3, 5.25, 4.75, 4.5, 4.2, 4, 4.15, 4.25, 4.3, 3.75, 3.95, 3.51, 4.13, 5.4, 5, 2.1, 4.6, 3.2, 2.5, 4.1, 3.5, 3.2, 3.3, 4.6, 4.3, 4.3, 4.5, 5.5, 4.6, 4.9, 4.3, 3, 3.4, 3.7, 4.4, 4.9, 4.9, 5.

The MLEs along with their corresponding SEs (shown in parentheses) are displayed in Table 6. The GoF results from the table show that the HT-W-EHL-W model fits the data better compared to its competitors.

The parameter estimates, obtained via MLE together with the SEs (in parentheses), are summarized in Table 6. Comparative GoF analysis reveals that the HT-W-EHL-W distribution provides a significantly closer approximation to the empirical fracture toughness of alumina data than alternative models, as evidenced by GoF statistics.

The 95% ACI for the parameters of the HT-W-EHL-W distribution are: $\alpha\in(0.8129\pm0.0999)$, $\beta\in(19.8660\pm1.3719\times10^{-03})$, $\theta\in(0.4587\pm0.4116)$, and $d\in(0.1971\pm0.2969)$, respectively. The parameters of the HT-W-EHL-W model on fracture toughness of alumina data are uniquely identifiable, as depicted in Figure 9.

The HT-W-EHL-W model exhibits exceptional concordance with the empirical data, as evidenced by graphical diagnostics. The fitted density plot (Figure 10) reveals remarkable alignment between the theoretical pdf and the observed data distribution, suggesting the model accurately captures the underlying data structure. This strong fit

Table 6. Fracture toughness of alumina data: Parameter estimates and GoF statistics

	Estimates				Statistics							
Distribution	α	β	θ	d	-2log(L)	AIC	CAIC	BIC	W^*	A^*	K−S	p−value
HT-W-EHL-W	0.8129	19.8660	0.4587	0.1971	335.8372	343.8372	344.1881	354.9537	0.0556	0.3805	0.0566	0.8402
	(0.0510)	(6.9997×10^{-04})	(0.2099)	(0.1515)								
	α	a	b	λ								
EHL-OBIII-LLoG	0.8341	0.0811	7.7467	2.3755	339.7134	347.7134	348.0642	358.8299	0.0597	0.4136	0.060	0.7787
	(0.6086)	(0.0460)	(6.5726)	(0.3232)								
	δ	a	b	λ								
RB-TIIEHL-TL-W	1.1029	4.9008×10^{05}	158.2500	0.1376	338.7672	346.7672	347.1181	357.8837	0.121	0.750	0.0807	0.4205
	(0.2426)	(1.3329×10^{-07})	(0.1044)	(5.1281×10^{-03})								
	α	λ	a	b								
OEHL-BXII	0.5061	8.2589×10^{-05}	5.0063	1.1710	389.9666	397.9666	398.3174	409.0830	0.1023	0.5912	0.0912	0.2757
	(398.4600)	(1.9029×10^{-05})	(6.1461×10^{-03})	(0.0279)								
	a	b	α	β								
KW	212.0600	1.1095×10^{-04}	281.2600	0.1597	340.1098	348.1098	348.4607	359.2263	0.1458	0.8999	0.0864	0.3365
	(8.7129×10^{-09})	(1.8487×10^{-10})	(3.4038×10^{-08})	(4.3424×10^{-04})								
	θ	α	β	λ								
TIHT-OPG-W-W	0.2043	3.8941	0.0396	1.6481	338.6788	346.6788	347.0297	357.7953	0.0576	0.3876	0.0584	0.8125
	(0.0819)	(8.2590)	(0.0.0840)	(0.2204)								
	β	λ	θ	γ								
ELOLLW	723.0600	0.5366	0.1071	3.2635	341.0091	349.0091	349.3600	360.1256	0.1556	0.9652	0.0859	0.3442
	$(4,0642 \times 10^{-06})$	(0.5289)	(0.3444)	(0.2309)								

is further confirmed by the ECDF plot in Figure 10, which demonstrates nearly perfect correspondence across the complete range of observed values. The K-M empirical survival curve in Figure 10 closely aligns with the fitted HT-W-EHL-W survival function, demonstrating the model's accuracy in capturing both central and extreme failure-time behavior. This strong visual agreement across the entire time domain, particularly in the right tail, confirms the model's robustness in characterizing the true survival pattern of the data.

The P-P plot in Figure 11 demonstrates excellent model fit, as evidenced by the close alignment of plotted points with the 45° reference line. This near-perfect correspondence between theoretical and empirical cumulative probabilities strongly validates the distributional assumptions of the HT-W-EHL-W model.

The TTT and hrf plots presented in Figure 11 reveal a consistently increasing hazard rate pattern for the fracture toughness of alumina data. This monotonic progression in the hazard function demonstrates that the risk of strand failure escalates with prolonged exposure to sustained stress loading conditions.

7.2. Bladder cancer data

The dataset includes the duration of remission (measured in months) for 137 patients diagnosed with bladder cancer. This data was initially used by Lee and Wang [13] and later by Gwazane et al. [11]. The dataset includes censored observations is presented as follows:0.08, 2.09, 3.48, 4.87, 6.94, 8.66, 13.11, 23.63, 0.20, 2.23, 3.52, 4.98, 6.97, 9.02, 13.29, 24.80∗, 0.40, 2.26, 3.57, 5.06, 7.09, 9.22, 13.80, 25.74, 0.50, 2.46, 3.64, 5.09, 7.26, 9.47, 14.24, 25.82, 0.51, 2.54, 3.70, 5.17, 7.28, 9.74, 14.76, 26.31, 0.81, 2.62, 3.82, 5.32, 7.32, 10.06, 14.77, 32.15, 0.87∗, 2.64, 3.88, 5.32, 7.39, 10.34, 14.83, 34.26, 0.90, 2.69, 4.18, 5.34, 7.59, 10.66, 15.96, 36.66, 1.05, 2.69, 4.23, 5.41, 7.62, 10.75, 16.62, 43.01, 1.19, 2.75, 4.26, 5.41, 7.63, 10.86∗, 17.12, 46.12, 1.26, 2.83, 4.33, 5.49, 7.66, 11.25, 17.14, 79.05, 1.35, 2.87, 4.33∗, 5.62, 7.87, 11.64, 17.36, 1.40, 3.02, 4.34, 5.71, 7.93, 11.79, 18.10, 1.46, 3.02∗, 4.40, 5.85, 8.26, 11.98, 19.13, 1.76, 3.25, 4.50, 6.25, 8.37, 12.02, 19.36∗, 2.02, 3.31, 4.51, 6.54, 8.53, 12.03, 20.28, 2.02, 3.36, 4.65∗, 6.76, 8.60∗, 12.07, 21.73, 2.07, 3.36, 4.70∗, 6.93, 8.65, 12.63, 22.69.

NB: The asterisk $(*)$ means censored data.

7.2.1. Bladder cancer data (Complete case): This subsection presents the MLEs with their corresponding SEs (reported in parentheses), GoF statistics, and diagnostic plots for the complete bladder cancer dataset. The results are systematically analyzed to assess model performance and validity.

The MLEs along with their corresponding SEs (shown in parentheses) are displayed in Table 7. The GoF results from the table show that the HT-W-EHL-W model fits the data better compared to its competitors. Table 7 summarises parameter estimates, obtained via MLE technique together with the SEs. Comparative GoF analysis reveals that the HT-W-EHL-W distribution provides significant approximation to the bladder cancer data compared to contending models, as evidenced by GoF statistics.

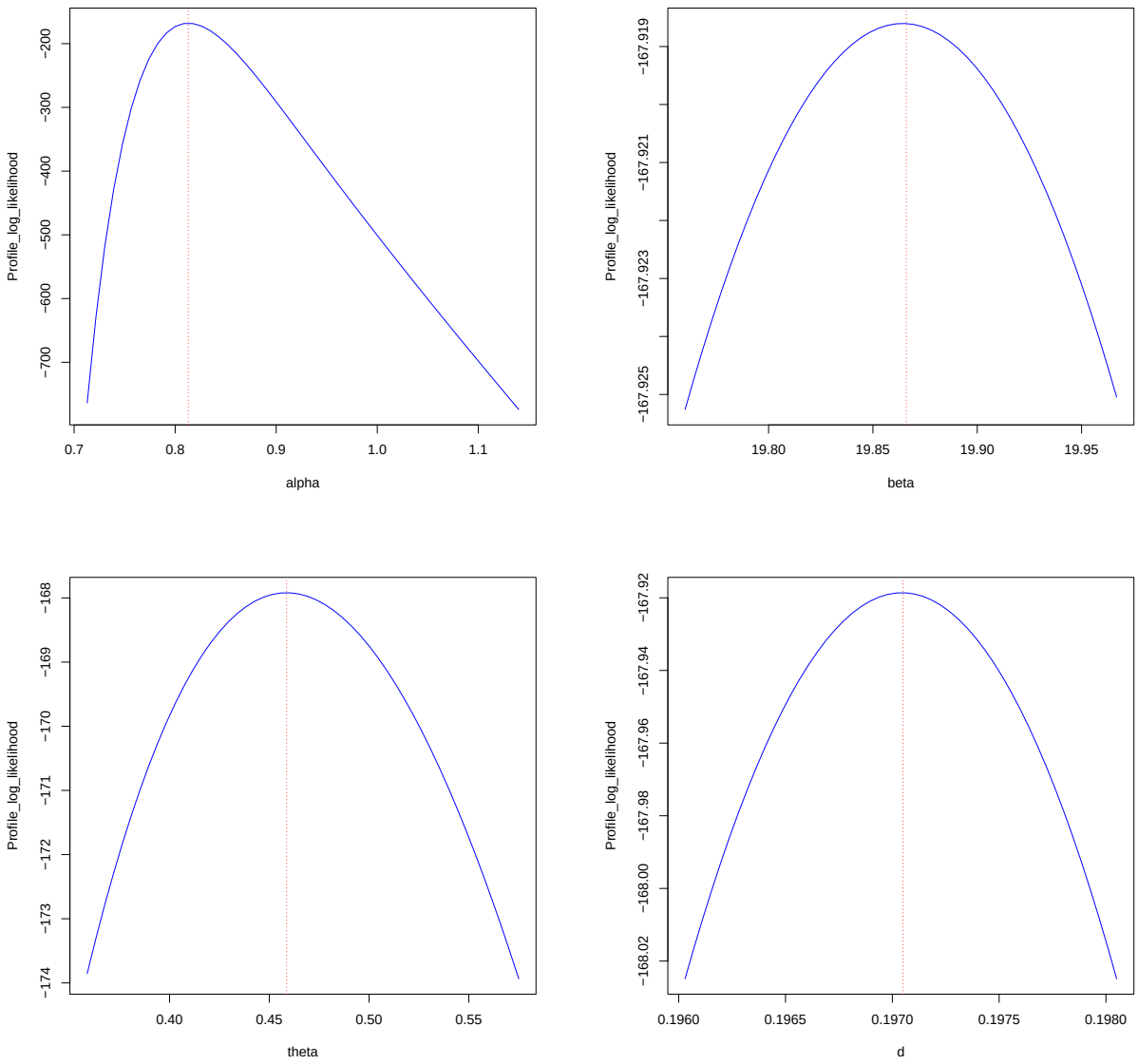

Figure 9. Profile log-likelihood plots for fracture toughness of alumina data

The 95% ACI for the parameters of the HT-W-EHL-W distribution are: $\alpha \in (5.5955 \pm 2.1264)$, $\beta \in (1.2839 \pm 0.8939)$, $\theta \in (3.8830 \pm 3.7393)$, and $d \in (2.4089 \pm 1.3339)$, respectively. The parameters of the HT-W-EHL-W model on bladder cancer data are uniquely identifiable, as depicted in Figure 12.

The HT-W-EHL-W model demonstrates excellent agreement with observed remission time data through graphical diagnostics. The fitted pdf (Figure 13) shows precise alignment with the histogram accurately capturing the characteristics of oncological data. This fit is also confirmed by the ECDF plot and K-M survival curves, where the model's theoretical distribution exhibits near-perfect concordance with observed remission probabilities across all time points.

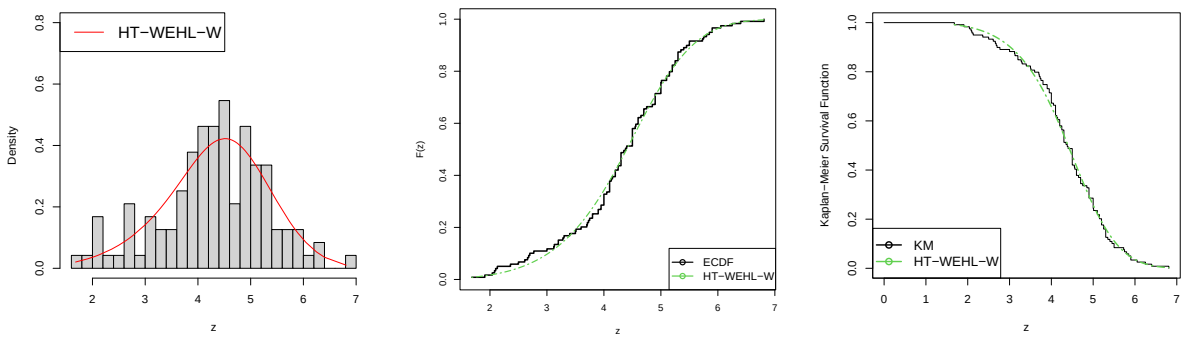

Figure 10. Graphs illustrating the fitted density plot, ECDF plot and the PP plot for fracture toughness of alumina data

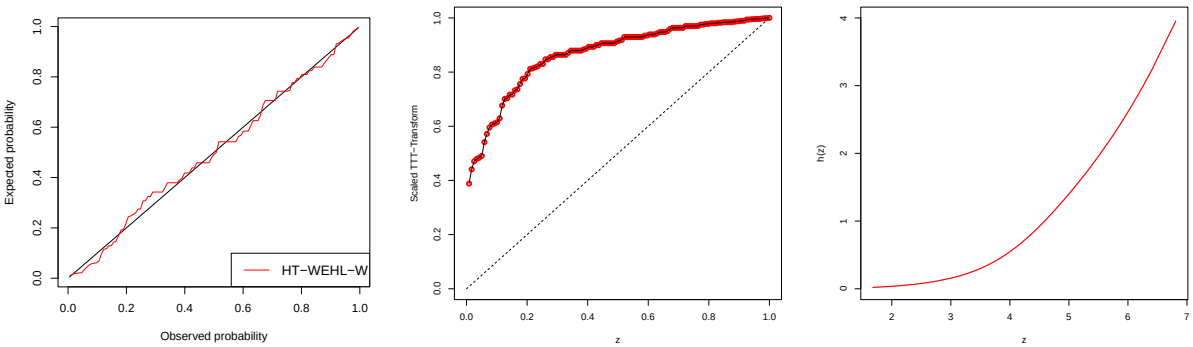

Figure 11. K-M survival curve, TTT scaled and hrf plots for fracture toughness of alumina data

Table 7. Bladder cancer data: Parameter estimates and GoF statistics

	Estimates				Statistics							
Distribution	α	β	θ	d	-2log(L)	AIC	CAIC	BIC	W^*	A^*	K−S	p−value
HT-W-EHL-W	5.5955	1.2839	3.8830	2.4089	820.1674	828.1674	828.4926	839.5755	0.0284	0.1919	0.0397	0.9876
	(1.0849)	(0.4561)	(1.9078)	(0.6805)								
	α	a	b	λ								
EHL-OBIII-LLoG	220.2900	1.4962	1.9439	5.3005×10^{-03}	843.2412	851.2412	851.5664	862.6494	0.2670	1.7367	0.0879	0.2761
	(2.1982×10^{-08})	(0.8556)	(0.9574)	(3.2357×10^{-04})								
	δ	a	b	λ								
RB-TIIEHL-TL-W	1.7370	4.9008×10^{05}	120.5402	0.0358	826.2534	834.2534	834.5786	845.6615	0.1080	0.6555	0.0666	0.6212
	(0.1581)	(2.0408×10^{-07})	(0.0147)	(1.6364×10^{-03})								
	α	λ	a	b								
OEHL-BXII	0.3025	0.0275	3.6829	0.3660	881.8121	889.8121	890.1373	901.2202	0.3274	1.9125	0.1166	0.0616
	(0.0649)	(0.0187)	(1.0211)	(0.0976)								
	a	b	α	β								
KW	42.8910	1.1097×10^{-04}	280.4700	0.0624	824.2797	832.2797	832.6049	843.6878	0.0868	0.5282	0.0595	0.7551
	(1.8680)	(2.7314×10^{-10})	(0.0234)	(2.8496×10^{-03})								
	θ	α	β	λ								
TIHT-OPG-W-W	6.1106	1.1125	2.08222×10^{-03}	1.1255	824.2596	832.2596	832.5848	843.6677	0.0879	0.5297	0.0604	0.7381
	(7.1359×10^{-04})	(0.2996)	(5.9627×10^{-03})	(0.0815)								
	β	λ	θ	γ								
ELOLLW	0.1002	0.1434	0.7185	1.0478	828.1738	836.1738	836.4990	847.5819	0.1314	0.7865	0.0700	0.5570
	(0.0988)	(7.6586)	(0.2125)	(0.0676)								

The P-P plot in Figure 11 demonstrates excellent model fit, as evidenced by the close alignment of plotted points with the 45° reference line. This near-perfect correspondence between theoretical and empirical cumulative probabilities strongly validates the distributional assumptions of the HT-W-EHL-W model.

The TTT and hrf plots presented in Figure 11 exhibit an inverted-bathtub hrf pattern in bladder cancer remission, showing an initial risk increase, followed by declining risk after. The model's ability to accurately capture this

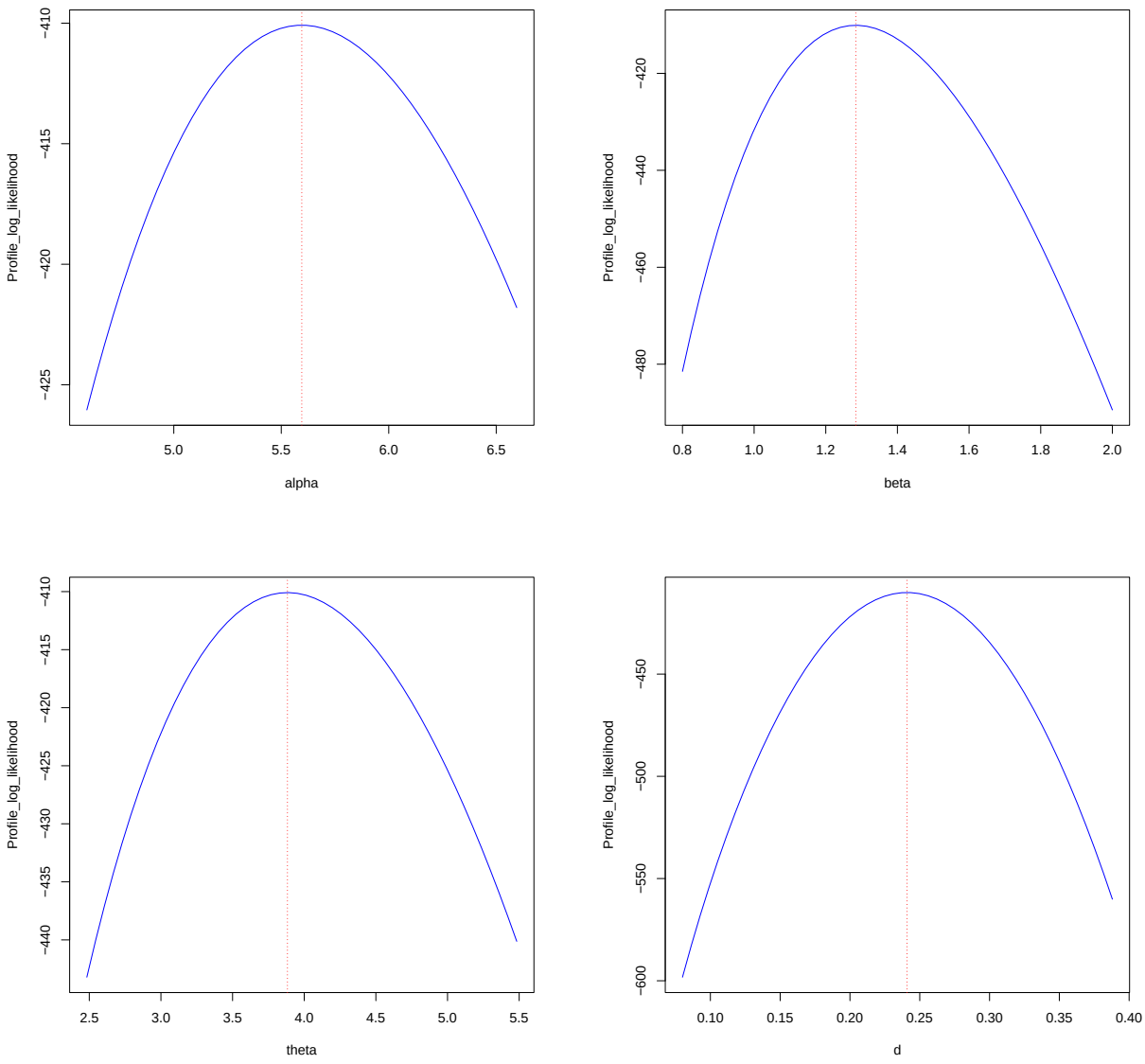

Figure 12. Profile log-likelihood plots for bladder cancer data

biphasic hazard pattern of bladder cancer remission with its early risk escalation and late-phase risk decline demonstrates its clinical utility for personalizing surveillance protocols, stratifying patient risk, and guiding therapeutic decisions, while statistically validating its robustness in modeling complex, non-monotonic survival behaviors.

7.2.2. Bladder cancer data (Censored case): This section contains parameter estimates and GoF statistics for bladder cancer censored data.

The 95% ACI for the parameters of the HT-W-EHL-W distribution fitted to the censored bladder cancer dataset are as follows: $\alpha \in (14.6588 \pm 0.2638)$, $\beta \in (0.5627 \pm 0.1827)$, $\theta \in (5.6945 \pm 6.1581)$, and $d \in (0.2088 \pm 0.1048)$, respectively.

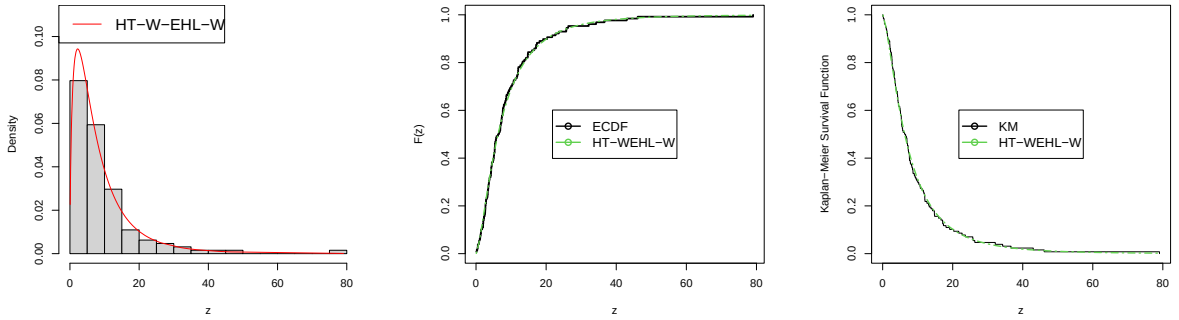

Figure 13. Graphs illustrating the fitted density plot, ECDF plot and the PP plot for bladder cancer data

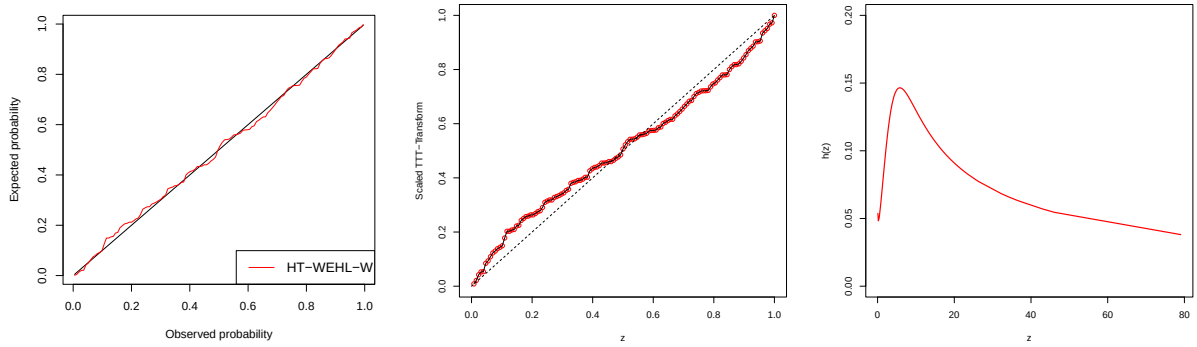

Figure 14. K-M survival curve, TTT scaled and hrf plots for bladder cancer data

Table 8. Bladder cancer data (Censored Case): Parameter estimates and GoF statistics

			Estimates		Statistics			
Distribution	α	β	θ	d	-2log(L)	AIC	CAIC	BIC
HT-W-EHL-W	14.6588	0.5627	5.6945	0.2088	837.4567	845.4567	846.5817	854.5505
	(0.1346)	(0.0932)	(3.1419)	(0.0535)				
	α	a	b	λ				
EHL-OBIII-LLoG	2.2100×10^{02}	1.4813	2.0091	0.0515	859.4506	867.4506	868.5756	876.5444
	(1.4757×10^{-08})	(0.8532)	(0.9943)	(3.1488×10^{-04})				
	δ	a	b	λ				
RB-TIIEHL-TL-W	7.0167	37.6341	110.9701	0.0883	841.5444	849.5444	850.6694	866.6382
	(0.3511)	(6.5839×10^{-03})	(0.0376)	(4.9621×10^{-03})				
	α	λ	a	b				
OEHL-BXII	0.3942	0.0223	3.6690	0.3782	897.0698	905.0698	906.1948	914.1636
	(0.0649)	(0.0187)	(1.0211)	(0.0976)				
	a	b	α	β				
KW	43.0670	1.1101×10^{04}	276.5500	0.0623	841.1507	849.1507	850.2757	858.2445
	(1.8715)	(2.7531×10^{-04})	(0.0238)	(2.8534×10^{-03})				
	θ	α	β	λ				
TIHT-OPG-W-W	5.9210	1.1113	2.0625×10^{-03}	1.1265	841.2852	849.2852	850.4102	858.3790
	(6.2044×10^{-04})	(0.2997)	(5.9139×10^{-04})	(0.0816)				
	β	λ	θ	γ				
ELOLLW	9.7330×10^{-07}	0.1321	0.7310	1.0536	844.8293	852.8293	853.9543	861.9232
	(0.1072)	(0.0216)	(3.7039×10^{-03})	(0.0681)				

8. Summary of Limitations Conclusions and recommendations

8.1. Limitations and Practical Considerations:

The HT-W-EHL-G model, while flexible, may present some key challenges including:

(i) Computational complexity: The model's multiple parameters can make maximum likelihood estimation slow and resource-intensive, especially with large datasets or censored data. Developing more efficient algorithms (for example, Expectation-Maximization) is needed for better scalability.
(ii) Risk of overparameterization: With four or more parameters, the model can become overly complex for smaller samples, leading to unstable estimates and poor predictions. Using model selection criteria (AIC, BIC) is crucial to avoid this pitfall.
(iii) Bayesian implementation hurdles: Applying Bayesian methods is difficult due to challenges in choosing appropriate priors for the complex parameter space and the need for advanced computational techniques like Markov Chain Monte Carlo (MCMC) to manage non-standard posterior distributions.

8.2. Conclusions and recommendations

The heavy-tailed Weibull exponentiated half logistic-G (HT-W-EHL-G) family of distributions provides a powerful and flexible framework for modeling complex data behaviors, including extreme events, skewness, and diverse hazard rates. Its superior performance, validated through extensive theoretical derivations and empirical testing, establishes a strong foundation for future advancements. Building on this foundation, several specific research avenues are particularly promising. Firstly, a bivariate extension of the family of distributions using copulas presents a direct and valuable direction for modeling complex dependencies between two random variables. Secondly, developing dedicated regression models for censored survival data would significantly enhance the model's utility in biostatistics, engineering, and reliability analysis. Furthermore, investigating Bayesian estimation methods would offer a robust alternative to maximum likelihood estimation by incorporating prior knowledge and providing a probabilistic framework for parameter uncertainty. Finally, continued computational optimizations of the estimation procedures will be crucial for handling large-scale datasets and facilitating the model's adoption in machine learning and big data analytics, thereby broadening its scope for interdisciplinary applications.

Appendix

To access the appendix, please click on the link provided below:
https://drive.google.com/file/d/1R3jQh9IB6_NViwwWQWusAW-liDCRZ4my/view?usp=sharing

Funding Statement

Thi s research did not receive any sponsorship from individuals or organizations.

Declaration of competing interest

The authors assert that there are no conflicts of interest among them.

REFERENCES

1. Afify, A. Z., Gemeay, A. M., and Ibrahim, N, A., *The heavy-tailed exponential distribution: risk measures, estimation, and application to actuarial data*, Mathematics, vol. 8, no. 8, pp. 1–28, 2020.

2. Aldahlan, M., and Afify, A. Z., *The odd exponentiated half-logistic Burr XII distribution*, Pakistan Journal of Statistics and Operation Research, vol. 12, no. 3, pp. 305–317, 2018.
3. Alzaatreh, A., Lee, C., and Famoye, F., *A new method for generating families of continuous distributions*, Metron, vol. 71, no. 1, pp. 63–79, 2013.
4. Arshad, M. Z., Iqbal, M. Z., and Al Mutairi, A., *A comprehensive review of datasets for statistical research in probability and quality control*, Journal of Mathematics and Computer Science, vol. 11, no. 3, pp. 3663–3728, 2021.
5. Charumbira, W. F., Oluyede, B., and Chipepa, F., *A new generalized gamma type II exponentiated half logistic-Topp-Leone-G family of distributions with applications*, Electronic Journal of Applied Statistical Analysis, vol. 17, no. 3, pp. 676–702, 2024.
6. Cheng, R. C. H., and Amin, N. A, K., *Maximum product of spacings estimation with applications to the log-normal distribution*, Technical report, Department of Mathematics, University of Wales, 1979.
7. Cheng, R. C. H., and Amin, N. A, K., *Estimating parameters in continuous univariate distributions with a shifted origin*, Journal of the Royal Statistical Society,vol. 45, no. 3, 1983.
8. Cordeiro, G. M., Alizadeh, M., and Ortega, E. M., *The exponentiated half-logistic family of distributions: properties and applications*, Journal of Probability and Statistics, vol. 2014, no. 1, 864396, 2014.
9. Cordeiro, G. M., Ortega, E. M. M., and Nadarajah, S., *The Kumaraswamy Weibull distribution with application to failure data*, Journal of the Franklin institute, vol. 347, no. 8, 2010.
10. Gradshteyn, I. S., and Ryzhik, I. M., *Table of integrals, series, and products*, Stats, vol. 6, no. 2, pp. 706–733, 2023.
11. Gwazane, M., Oluyede, B., and Chipepa, F., *The new family of exponentiated half logistic-type I heavy-tailed-G distributions with applications*, Electronic Journal of Applied Statistical Analysis, vol. 18, no. 1 pp. 102–132, 2025.
12. Korkmaz, M., Yousof, H. M. and Hamedani, G. G., *The exponential Lindley odd log-logistic-G family: properties, characterizations and applications*, Journal of Statistical Theory and Applications, vol. 17, no. 3, pp. 554–571, 2018.
13. Lee, E. T., and Wang, J., *Statistical methods for survival data analysis*, John Wiley & Sons, vol. 476, 2003.
14. Moakofi, F., and Oluyede, B., *The type I heavy-tailed odd power generalized Weibull-G family of distributions with applications*, Communications Faculty of Sciences University of Ankara Series A1 Mathematics and Statistics, vol. 72, no. 4, pp. 921–958, 2023.
15. Moakofi, T., Oluyede, B., Puoetsile, A., and Warahena-Liyanage, G., *A new generalized family of Weibull-exponentiated half Logistic-G distribution with applications*, Central European Journal of Economic Modelling and Econometrics, vol. 17, no. 3, pp. 125–189, 2024.
16. Nkomo, W., Oluyede, B. and Chipepa, F., *Topp-Leone type I heavy-tailed-G power series class of distributions: properties, risk measures, and applications*, Statistics, Optimization and Information Computing, vol. 13, no. 1, pp. 88–110, 2025.
17. Nkomo, W., Oluyede, B. and Chipepa, F., *Type I heavy-tailed family of generalized Burr III distributions: Properties, actuarial measures, regression and applications*, Statistics in Transition New Series, vol. 26, no. 1, pp. 93–115, 2025.
18. Oluyede, B., Ookame, P. P., Ndwapi, N., and Bindele, H., *The exponentiated half-logistic odd Burr III-G: Model, properties and applications*, Pakistan Journal of Statistics and Operation Research, vol. 33, no. 2, pp. 33–57, 2022.
19. Oluyede, B., Ookame, P. P., Ndwapi, N., and Bindele, H., *The Weibull exponentiated half logistic-G family of distributions with properties and applications*, Statistics in Transition new series (In review).
20. Rényi,A., *On measures of entropy and information*, Proceedings of the Fourth Berkeley Symposium on Mathematical Statistics and Probability, vol. 1, pp. 547–561, 1960.
21. Shannon, C. E., *Prediction and entropy of printed english*, The Bell System Technical Journal, vol. 30, pp. 50–64, 1951.
22. Tahir, M. Z., Hussian, M., Mansoor, M., Cordeiro, G.M., Alizadehk, M., and Hamedani G., *A new Weibull-G family of distributions*, Hacettepe Journal of Mathematics and Statistics, vol. 45, no. 2, pp. 629–647, 2016.
23. Teamah, A. A. M., Elbanna, A. A., and Gemeay, A. M., *Heavy-tailed log-logistic distribution: Properties, risk measures and applications*, Statistics, Optimization & Information Computing, vol. 9, no. 4, pp. 910–941, 2021.
24. Warahena-Liyanage, G., Oluyede, B., and Moakofi, T., *The new Ristić-Balakrishnan-heavy-tailed-type II Topp-Leone-G family of distributions with applications*, Journal of Statistical Theory and Applications, vol. 6, no. 2, pp. 1–40, 2025.
25. Zhao, J., Ahmad, Z., Mahmoudi, E., Hafez, E. H. H., and Marwa, M. M. E., *A new class of heavy-tailed distributions: Modeling and simulating actuarial measures*, Complexity, vol. 2021, no. 1, 5580228, 2021.
26. Zhao, W., Khosa, S. K., Ahmad, Z., Aslam, M., and Afify, A. Z., *The type-I heavy tailed family with applications in medicine, engineering and insurance*, PloS One, vol. 15, no. 8, e0237462, 2020.